Ferdowsi University of Mashhad
ISSN 2008-9147
Numbers: 9

JCMR

Journal of Cell and Molecular Research

Volume 5, Number 1, Summer 2013

بسم الله الرحمن الرحيم

Issuance License No. 124/902-27.05.2008 from Ministry of Culture and Islamic Guidance
Scientific Research Issuance License No. 161675 from the Ministry of Science, Research and Technology, Iran

Journal of Cell and Molecular Research (JCMR)

Volume 5, Number 1, Summer 2013

Office: Department of Biology, Faculty of Sciences, Ferdowsi University of Mashhad, Mashhad, Iran.
Postal Code: 9177948953
P.O. Box: 917751436
Tel./Fax: +98-511-8795162
E-mail: fuijbs@um.ac.ir
Online Submission: http://jm.um.ac.ir/index.php/biology

Table of Contents

The Editorial

Stem Cells of Epidermis: A Critical Introduction

Stem cells are the cells having some distinguishing characteristics like longevity, high capacity of self-renewal and differentiation, quiescence and highly error-free proliferation. Almost all stem cells have the potential of lineage reprogramming, i.e. inter-conversion of cell lineages. They also have the potential to differentiate into almost all kinds of cells. These cells have been found in almost every organs of human body. Pool of stem cells found in epidermis is termed as Epidermal Stem Cells (Blanpain and Fuchs, 2006).

Many researchers around the world have reported different kinds of stem cells in skin, based on their cell surface makers, while they have not categorized these cells chronically (De Rosa and De Luca, 2012). It is worth mentioning here that all kinds of stem cells reported in skin, i.e. keratinocyte stem cells, limbal stem cells, hair follicle and bulge stem cells, SG (sebaceous gland) stem cells, and spinous keratinocytes express specific types of cytokeratin protein (e.g. K1, K3, K5, K10, K12, K14, K15, K19 etc.) on their surfaces (Bose et al., 2013; Forni et al., 2012; Ghadially, 2012).

Biologists have defined that almost all of these stem cells share single origin, i.e. Basal Layer of Embryonic Skin. As the embryonic skin passes the developmental stages, the basal layer produces two mother stem cells of skin, keratinocyte stem cells, and so called Limbal Stem Cells (in cornea) (Chee et al., 2006; Lavker and Sun, 2000).

Keratinocyte stem cells give rise to the cells expressing Cytokeratin proteins on their surfaces. So, all the cells expressing cytokeratin are tracked back to these stem cells in origin , while undergone natural lineage reprogramming or differentiation (Potten and Booth, 2002). The stem cells in the basal-layer give rise to keratinocyte stem cells which can be found in the basal layer of the adult skin (Kaur et al., 2004). During the developmental stages, this basal layer, containing keratinocyte stem cells, gives rise to limbal invagination of corneal region, a linage conversion mechanism happens, and the keratinocyte stem cells are naturally reprogramed into the limbal stem cells as shown in figure 1 (Dua and Azuara-Blanco, 2000; Pellegrini et al., 2001).

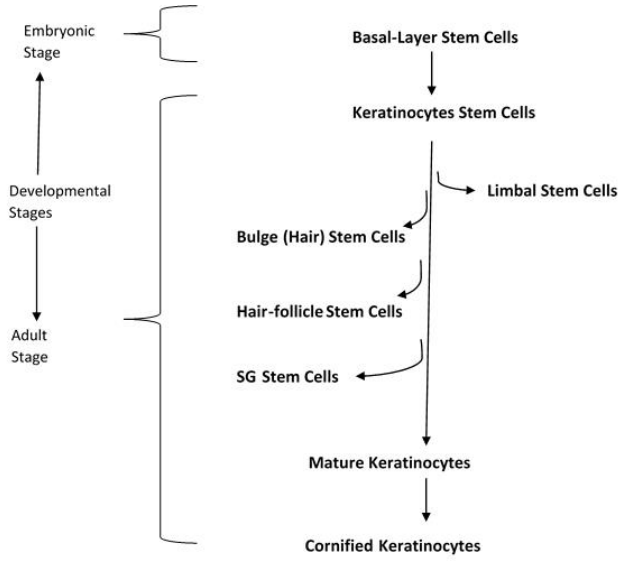

Figure 1: Proposed hierarchy of epidermal stem cells

In basal layer of the epidermis, the keratinocyte stem cells give rise to bulge, hair follicle, and SG stem cells when placode formation takes place.

In future, we need studies to find out which kind of cytokeratin protein is expressed early in these cells. In another word it would be helpful to define the order of cytokeratin expression regarding these lineage developmental processes from embryonic to mature skin and from embryonic basal layer to the formation of cornified epithelial cells.

References:

1- Blanpain C. and Fuchs E. (2006) Epidermal stem cells of the skin. Annual review of cell and developmental biology 22:339-373.
2- Bose A., Teh M. T., Mackenzie I. C. and Waseem A. (2013) Keratin k15 as a biomarker of epidermal stem cells. International journal of molecular sciences 14:19385-19398.
3- Chee K. Y., Kicic A. and Wiffen S. J. (2006) Limbal stem cells: the search for a marker.

∗Corresponding author E-mail:
Muhammad Irfan-Maqsood
Managing Editor, JCMR
muhammadirfanmaqsood@gmail.com

Clinical & experimental ophthalmology 34:64-73.

4- De Rosa L. and De Luca M. (2012) Cell biology: Dormant and restless skin stem cells. Nature 489:215-217.

5- Dua H. S. and Azuara-Blanco A. (2000) Limbal stem cells of the corneal epithelium. Survey of ophthalmology 44:415-425.

6- Forni M. F., Trombetta-Lima M. and Sogayar M. C. (2012) Stem cells in embryonic skin development. Biological research 45:215-222.

7- Ghadially R. (2012) 25 years of epidermal stem cell research. The Journal of investigative dermatology 132:797-810.

8- Kaur P., Li A., Redvers R. and Bertoncello I. (2004) Keratinocyte stem cell assays: an evolving science. The journal of investigative dermatology. Symposium proceedings / the Society for Investigative Dermatology, Inc. [and] European Society for Dermatological Research 9:238-247.

9- Lavker R. M. and Sun T. T. (2000) Epidermal stem cells: properties, markers, and location. Proc Natl Acad Sci U S A 97:13473-13475.

10- Pellegrini G., Dellambra E., Golisano O., Martinelli E., Fantozzi I., Bondanza S., Ponzin D., McKeon F. and De Luca M. (2001) p63 identifies keratinocyte stem cells. Proc Natl Acad Sci U S A 98:3156-3161.

11- Potten C. S. and Booth C. (2002) Keratinocyte stem cells: a commentary. The Journal of investigative dermatology 119:888-899.

Cloning, nucleotide sequencing and bioinformatics study of NcGRA7, an immunogen from *Neospora caninum*

Mahdi Soltani[1], Mohammadreza Nassiri[1,2]*, Alireza Sadrebazzaz[3], Mojtaba Tahmoorespoor[1,2]

1 - Department of Animal Sciences, College of Agriculture, Ferdowsi University of Mashhad, Mashhad, Iran.
2 - Agricultural Biotechnology Research Group, Institute of Biotechnology, Ferdowsi University of Mashhad, Mashhad, Iran.
3 - Razi Serum and Vaccine Research Institute, Mashhad, Iran

Received 20 July 2013 Accepted 01 September 2013

Abstract

Neospora caninum is an obligate intracellular parasitic protozoa and considered as causal agent of Neosporosis which infect wide variety of hosts. NcGRA7 is an immunodominant antigen recognized by sera from bovines, naturally infected by *N. caninum*, which is used as a powerful target for recombinant or DNA vaccine preparation against neosporosis. There is no study about identifying the molecular structure of *Neospora caninum* in Iran, so as first step, current study tried to identify NcGRA7 gene in this parasite in Iran. After extraction of total RNA from *N. caninum* tachyzoites, cDNA was synthesized and NcGRA7 gene was amplified using cDNA as template. Then the PCR product was cloned into pTZ57R/T vector and transformed into *Escherichia coli* (DH5α strain), and the resulted recombinant plasmid was submitted for sequencing, followed by bioinformatics analysis. The data obtained from sequencing of native NcGRA7 was recorded in GenBank. The deduced amino acid sequence of NcGRA7 in current study was compared with other *N. caninum* NcGRA7 sequences and showed some identities and differences. NcGRA7 gene of *N. caninum* was successfully cloned into the pTZ57R/T vector and recombination was confirmed by sequencing, colony PCR, and enzymatic digestion, making it ready expression of recombinant protein for further studies.

***Keywords*:** *Neospora caninum*, NcGRA7, Cloning, Sequencing

Introduction

Bovine neosporosis is the most frequently diagnosed cause of bovine abortion worldwide (Monney et al., 2011). *Neospora caninum*, a persistent protozoan parasite capable of infecting almost any warm-blooded vertebrate, is a member of phylum apicomplexa and has a complex lifestyle involving two phases of growth: an intestinal phase in canine hosts, and an extra-intestinal phase in other mammals (Dubey and Schares, 2011). It was originally identified in tissues of paralyzed dogs (Bjerkas and Presthus, 1988; Dubey et al., 1988). As revealed by molecular analyses, *N. caninum* is closely related to other coccidian parasite, *Toxoplasma gondii*, and therefore many of previously described *T. gondii* biological characteristics can be attributed to *N. caninum* so they would employ similar mechanisms for adhesion and invasion processes (Monney et al., 2011). Results of studies on *Neospora caninum* infection in Iran showed that this parasite could be considered as a cause of economic loss in dairy cattle (Salehi et al., 2009). From several areas in Iran, Neospora infection has been reported in cattle (Nematollahi et al., 2011; Nourollahi Fard et al., 2008; Razmi et al., 2006; Sadrebazzaz et al., 2007; Sadrebazzaz et al., 2004), dogs (Haddadzadeh et al., 2007; Hosseininejad et al., 2010; Malmasi et al., 2007; Yagoob, 2011) and camels (Hosseininejad et al., 2009; Sadrebazzaz et al., 2006).

Current studies on *N. caninum* are mainly focused on the mechanisms and antigens involved in the tachyzoite adhesion, invasion and its proliferation and persistence in the host cell and using these antigens for immunological purposes (Dubey and Schares, 2011). NcSRS2 was one of the most worked targets for developing recombinant vaccines and diagnostic kits against neosporosis (Soltani et al., 2013).

N. caninum exploits different secretory and antigenic proteins to invade a host cell and gain access to its intracellular environment. These proteins originate from distinct organelles termed micronemes, rhoptries, and dense granules. They are released at specific times during invasion to ensure the proteins are allocated to their correct target destinations(Howe and Sibley, 1999). Dense granule antigens (GRAs) are secreted by dense granules to the parasitophorous vacuole during parasite intracellular development (Cesbron-delauw, 1994). Dense-granule secretion shares several features with the regulated secretory

*Corresponding author E-mail:
nassiryr@gmail.com

pathway: (1) packaging in electron-dense vesicles; (2) fusion of these vesicles with the plasma membrane; and (3) calcium-regulated exocytosis. It has been suggested that dense granule antigens stimulate humoral immunity in the host. GRA7 is a highly immunogenic, dense granule protein in both T. gondii and *N. caninum* (Lally et al., 1997; Vonlaufen et al., 2004). Moreover, although GRA proteins appear to be related to intracellular parasite development, previous studies revealed that NcGRA7 might be involved in the initial host cell invasion process of *N. caninum* (Augustine et al., 1999; Cho et al., 2005). It has been showed that this immunogenic protein provides some protection against experimental *N. caninum* infection (Jenkins et al., 2004; Liddell et al., 2003; Nishikawa et al., 2009). Thus, the NcGRA7 protein could be considered as a vaccine candidate against neosporosis. Moreover, the immunogenicity of NcGRA7 has led to investigation of this antigen as a diagnostic reagent (Huang et al., 2007).

In the framework of the investigations on designing recombinant vaccines against neosporosis, this work focuses on the cloning and sequencing of NcGRA7 from Iranian isolate of *N. caninum* for the first time and bioinformatics based characterization of the important properties of its deduced protein. This work is first step in an attempt to design vaccine studies against neosporosis using NcGRA7 antigen that will be studied in the future.

Materials and Methods

Production of N. caninum tachyzoites

All cell culture reagents were purchased from Gibco-BRL (Zurich, Switzerland) and chemicals were from Sigma (St. Louis, MO, USA). Vero cells were routinely cultured in 25 cm2 tissue culture flasks in 5 ml of RPMI 1640 medium supplemented with 10% heat-inactivated FCS, 2 mM glutamine, 50 U of penicillin / mL and 50 ug of streptomycin / ml and incubated at 37ºC with 5% CO2. A strain of *Neospora caninum* was kindly provided by Dr. Sadrebazzaz (Razi vaccine and serum research institute, Mashhad branch). *N. caninum* cells were maintained in BALB/c mice by serial intraperitoneal inoculation of parasites was used for the experiment. *N. caninum* tachyzoites was maintained by serial passages in Vero cells. Cultures were passaged at least once per week. When 80% of the Vero cells that had been infected with *N. caninum* tachyzoites shows cytopathic effect (typically 3-4 days p.i.), the cell monolayers were removed by scraping, twice washed with phosphate buffered saline (PBS) solution, and then centrifuged at 1000 g for 10 min. Purified tachyzoites were checked for viability using trypan blue staining. Infected cells were trypsinized, washed twice in cold RPMI 1640 medium and the resulting pellet resuspended in 2 ml cold RPMI 1640 medium. Cells were repeatedly passed through a 25G needle.

RNA isolation and first strand cDNA synthesis

Total RNA was isolated from 2 × 106 purified *N. caninum* tachyzoites using NucleoSpin® RNA II kit (Machery-Nagel, Germany) according to the manufacturer's instructions using gene specific primers. RNA concentration was measured with the NanoDrop ND1000 (Thermo Scientific, Delaware, US) system.

Single-stranded cDNA was synthesized from isolated total RNA using a cDNA synthesis kit (RevertAid™ First Strand cDNA Synthesis Kit, Fermentas, Germany) according to the standard protocol for first strand cDNA synthesis. Briefly, first strand cDNA synthesis reaction was performed in a 20 µl reaction mixture containing 100 ng of total RNA, 4 µl 5X reaction buffer, 2 µl 10 mM dNTP Mix, 12 µl nuclease-free water, 1 µl RiboLock™ RNase Inhibitor (20 u/µl), 1 µl RevertAid™ M-MuLV Reverse Transcriptase (200 u/µl) and 15 pmol of each gene specific primers. Reaction mixtures were incubated for 5 minutes at 25 °C followed by 60 minutes at 42 °C and the reactions were terminated by heating at 70 °C for 5 minutes.

PCR amplification

A pair of gene-specific primers were designed using Primer Premiere software (Biosoft) based on published NcGRA7 gene sequence in the GenBank to amplify NcGRA7 gene. Primers were synthesized by as follows: NG71-F (5´-CGAGAATTCAAAATGGCCCGACAAGC-3´) and NG71-R (5´-CGCAGGATCCTAACTATTCGGTGTCTAC-3´) (Bioneer, South Korea). PCR reactions were performed using total cDNA as template. Reaction was carried out in 25 µl volume containing approximately 100 ng of cDNA template, 50 mM Tris buffer (pH: 8.3), 1.5 mM MgCl2, 200 mM of each ddNTPs, 0.5 U of Pfu DNA polymerase and 100 pM of each primers. Amplification reaction was performed using the following thermal profile: 95°C for 5 min, 35 amplification cycles (94°C for 40 sec, 62.5°C for 40 sec, and 72°C for 40 sec.), followed by a 72°C final extension for 10 min. Furthermore, false-negative results, caused by inhibitory compounds in the PCR reactions, were

excluded by performing a simultaneous positive control reaction using the DNA extracted from tachyzoites of the NC-1 strain. The negative control consisted of dH2O without DNA. A positive and negative control was included in each reaction. Amplified PCR products were analyzed by electrophoresis of 5 µl of each sample on 1% (W/V) agarose gel at a constant voltage of 100 v for 40 minutes, stained with SYBR® Safe DNA Gel Stain (Invitrogen, Paisley, UK). GeneRulerTM 100 bp Plus DNA Ladder (Fermentas) was used to compare the DNA fragment sizes. Agarose gel illuminated under UV, and photographed with an UVidoc Gel Documentation System (UVitec, UK).

Gel extraction of PCR products

The specific amplimers containing desired gene sequence were purified from the agarose gel by QIAquick Gel Extraction Kit (Qiagen, Germany) based on manufacturer's recommendations. This kit follows a simple bind-wash-elute procedure. Gel slices were dissolved in a buffer containing a pH indicator, allowing easy determination of the optimal pH for DNA binding, then mixtures were applied to the QIAquick spin column. Nucleic acids adsorbed to the silica membrane in the conditions provided by the buffer. Impurities were washed away and pure DNA was eluted with a small volume of low-salt buffer provided.

A tailing of PCR products

As exonuclease activity of the proofreading polymerases removes the 3´-A overhangs necessary for TA cloning, 3´-A overhangs must be added to fragments taking advantages of non-template activity of Taq DNA polymerase after PCR amplification since Taq polymerase preferentially adds an A to the 3'-ends in the presence of all four dNTPs. Briefly, a reaction was set up containing 25 µl purified PCR product, 5 µl 10X Taq reaction buffer, 5 µl MgCl2, 5 µl dNTP (10 mM stock), 1 µl Taq polymerase, 9 µl H2O. Then the mixture was incubated at 70 ºC for 30 min. Finally, 3 µl of reaction mixture was run on a gel to quantify. This reaction product can directly be used in ligation reaction without any need to clean up reaction.

Ligation into pTZ57R/T vector

Tailed PCR products were ligated into pTZ57R/T Vector (Fermentas, Germany) based on TA cloning scheme according to the manufacturer's instructions. A 1:3 (vector to insert) molar ratio was used. Ligation reaction sat up in 30 µl volume containing 3 µl pTZ57R/T plasmid, 10 µl of A tailed PCR product, 1 µl T4 DNA ligase enzyme, 6 µl 5X buffer and 10 µl nuclease free distilled water. After gentle mix and a brief centrifuge, the ligation reaction mixture was incubated overnight at 10ºC. The resulting plasmid was designated as pTZ-NcGRA7. Recombinant vector were stored at -20°C until transformation.

Transformation, Screening and Colony PCR

Preparation of competent cells from Escherichia coli strain DH5-α was performed by calcium chloride method (Sambrook et al., 1989). Advantages of chemical preparation of competent cells include simple procedure; no special equipment required and gives good transformation efficiencies. In general, it is the best method to use when the transformation efficiencies is not the problem. For transformation, 10 µl of ligation reaction product was added to 150 µl of competent cells and placed on ice for 40 minutes after vortex and spin. Then the mixture was incubated at 42 ºC for 90 s and immediately was placed on ice for 5 minutes. Then 1 ml of LB antibiotic free medium was added to the transformed cells and allowed to recover by incubation at 37 ºC for 2 hours with shaking. Cells harboring pTZ-NcGRA7 plasmid was plated and grown overnight at 37 ºC on a LB agar plate (10 g NaCl, 5 g yeast extract, 10 g bacto tryptone) with ampicillin (100 µg/ml), X-Gal (Fermentas) and IPTG (Fermentas) for blue-white screening. After overnight incubation, plate was placed at 4 ºC for 2 hours and cells from white colonies were harvested and cultured on antibiotic containing LB agar plates. After 16 hours incubation at 37 ºC, cells harboring the recombinant plasmid grew up. Recombination confirmed by colony PCR with NcGRA7 gene specific primers. This technique was used to determine insert size in the vector. Briefly, a colony was picked with toothpick and swirl into 50 µl of ddH2O in 1.5 ml microfuge tube. Then the tubes were heated at 95 ºC for 10 minutes. Tubes were centrifuged for 5 minutes at top speed in microfuge and 40 µl of supernatant was transferred to 0.5 ml microfuge tubes and 2 µl of it was used as template in PCR reaction. All other PCR reactions conditions were as explained before.

Plasmid Purification

Cells harboring the recombinant plasmid were cultured in antibiotic containing LB medium for 16 hours at 37 ºC in a shaker incubator. GeneJET Plasmid Miniprep Kit (Fermentas) was used to purify plasmids from E. coli DH5α following the manufacturer's instructions. Briefly, 4 ml bacterial culture was harvested and lysed. The lysate was then cleared by centrifugation and applied on the silica column to selectively bind DNA molecules.

The adsorbed DNA was washed to remove contaminants, and the pure plasmid DNA was eluted in a small volume of elution buffer. Plasmid DNA concentrations were determined by absorbance at 260 nm using NanoDrop ND1000 (Thermo Scientific, Delaware, US) system. The integrity of the DNA plasmids was checked by agarose gel electrophoresis. Also resultant recombinant plasmid (pTZ-NcGRA7) was compared with native plasmid (pTZ57R/T) by electrophoresis of 3 µl of extracted plasmid on a 1% agarose gel.

Enzymatic Digestion of pTZ-NcGRA7

With regard to presence of BamHI and EcoRI restriction sites on recombinant plasmid extracted from white colonies, the recombinant plasmid was characterized for the presence and size of inserts by double digestion with *Eco*RI and *Bam*HI. Each 20 µl digestion reaction contained 10 µl of plasmid, 1 µl of each restriction enzyme, 2 µl of 10X buffer (buffer R, based on Fermentas recommendations) and 6 µl of dH2O. Digestion was performed by incubation at 37 ºC for 2 hours. Digestion products were analyzed by electrophoresis on 1% agarose gel containing SYBR® Safe DNA Gel Stain (Invitrogen, Paisley, UK).

Sequencing of NcGRA7 gene

The nucleotide sequence of the inserts (NcGRA7) in the recombinant plasmid pTZ-NcGRA7 was verified by sequencing in the forward and reverse directions using primer walking approach (Eurofins MWG Operon, Germany). M13 uni (-21) forward primer (5´-TGTAAAACGACGGCCAGT-3´) and M13 rev (-29) reverse primer (5´-CAGGAAACAGCTATGACC-3´) were used for sequencing. DNA Baser v3 (Heracle BioSoft, Romania) was used for sequencing data assembly to produce a consensus sequence for each DNA sample used.

Blast search and bioinformatics study

The nucleotide sequence of NcGRA7 was submitted to the BLAST search (megablast algorithm) at NCBI server (http://www.ncbi.nlm.nih.gov/blast/) to compare with sequences presented in the GenBank. For detailed analysis, all closely related sequences and deduced amino acid sequences between published sequences were aligned by ClustalW2 multiple sequence alignment program (http://www.ebi.ac.uk/Tools/clustalw2/) (Larkin et al., 2007).

The sequences were analyzed for signal peptides using SignalP 4.0 (http://www.cbs.dtu.dk/services/SignalP/) (Petersen et al., 2011), protein domains using Prosite (http://prosite.expasy.org/) (Sigrist et al., 2010) and potential transmembrane regions were checked with the ProtScale tool on the Expasy server (http://expasy.org/tools/protscale.html).

Hydrophobicity plot of NcGRA7 protein was also drawn which characterizes its hydrophobic and hydrophilic characteristics that may be useful in predicting membrane-spanning domains, potential antigenic sites and regions that are likely exposed on the protein surface (Hopp and Woods, 1981; Kyte and Doolittle, 1982).

Phylogenetic and molecular evolutionary analyses were conducted using CLC main workbench software (CLC bio) by bootstrap test with 1000 replications was applied to estimate the confidence of branching patterns of the UPGMA tree. Also, pairwise comparisons were done to clarify the pairwise distances and percent identities.

Results

Production of N. caninum tachyzoites

Vero cells became confluent on day 3 and then were infected with *Neospora caninum* tachyzoites. Tachyzoites grew well in Vero monolayers (Fig. 1). *N. caninum* tachyzoites were maintained in and purified from, Vero cell monolayers and were immediately used for RNA extraction.

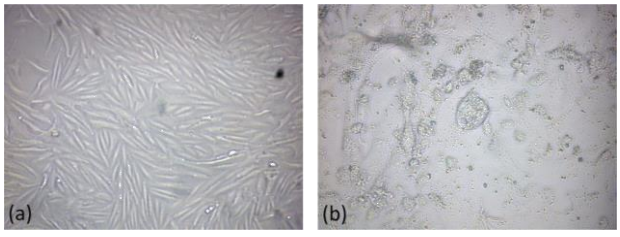

Figure 1. (a) Confluent Vero cells on day 3. **(b)** *N. caninum* tachyzoite infected Vero cells.

RNA isolation and first strand cDNA synthesis

Extracted RNA samples had very good quality and integrity based on Nanodrop analysis results. The OD 260/280 ratio for purified RNA was between 1.80–1.95, indicating that preparations were free of any major protein contamination. NanoDrop results showed that first strand cDNA synthesis reaction was successful.

PCR amplification

As PCR results showed, synthesized cDNA was successfully amplified by PCR reaction. The

presence of amplicons is characteristic for the presence of the *N. caninum* DNA. Length of NcGRA7 specific product was about 679 bp. The intensity and size of bands was identical with *N. caninum* (NC-1) positive controls that confirmed the accuracy of performed reactions. Furthermore, no visible bands can be seen in negative control lanes. PCR products were used for ligation into pTZ57R/T vector after A-tailing process.

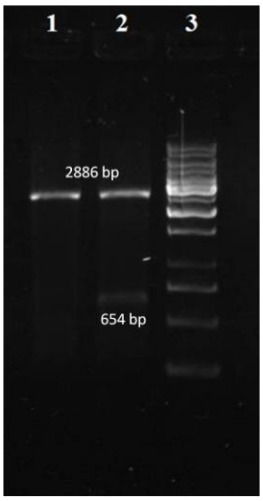

Figure 2. Agarose Gel electrophoresis of restriction enzyme digested recombinant plasmid pTZ-NcGRA7. lane 1: native pTZ57R/T, lane 2: EcoRI/BamHI digested pTZ-NcGRA7, lane 3: 1 kb DNA size marker.

Comparison of native and recombinant plasmids

A-tailed PCR products were successfully ligated into pTZ57R/T vector by TA cloning scheme. Resultant recombinant plasmid (pTZ-NcGRA7) was compared with native pTZ57R/T by electrophoresis on 1% agarose gel. As expected, pTZ-NcGRA7 (3540 bp length) was longer than native pTZ57R/T (2886 bp). Different bands revealed in each plasmid lane can be attributed to different forms of extracted plasmid DNA (linear, open circular and supercoil).

Colony PCR and Enzymatic digestion

Colony PCR was used to confirm recombination with NcGRA7 gene specific primers. All PCR reaction conditions were as before. Selected white colonies generated strong bands after PCR that showed recombination process was done as expected.

To further confirm presence and size of insert in pTZ-NcGRA7, recombinant plasmid was simultaneously digested with two enzymes (EcoRI/BamHI). After electrophoresis of digestion reaction on 1% agarose gel, 2 bands were detected in each lane that can be attributed to pTZ57R/T band (2886 bp) and insert band (654 bp for NcGRA7). As shown in Fig. 2, an insert with expected length was detected.

Sequencing of NcGRA7

PCR generated NcGRA7 gene was successfully cloned and sequenced. Sequence data reported in this paper is available in the GenBank database under the accession number JQ410455. Based on the in silico estimates using CLC main workbench software package (CLC bio), protein encoded by NcGRA7 gene had length of 217 amino acids with the calculated molecular mass of 22 kDa (Fig. 3) which was similar to the NcGRA7 protein sequences obtained from the *Neospora caninum* homepage on GeneDB (http://www.genedb.org/Homepage/Ncaninum). The protein corresponds to the following gene model as NCLIV_021640.

Bioinformatics study

Blast analysis of NcGRA7 gene revealed 100%

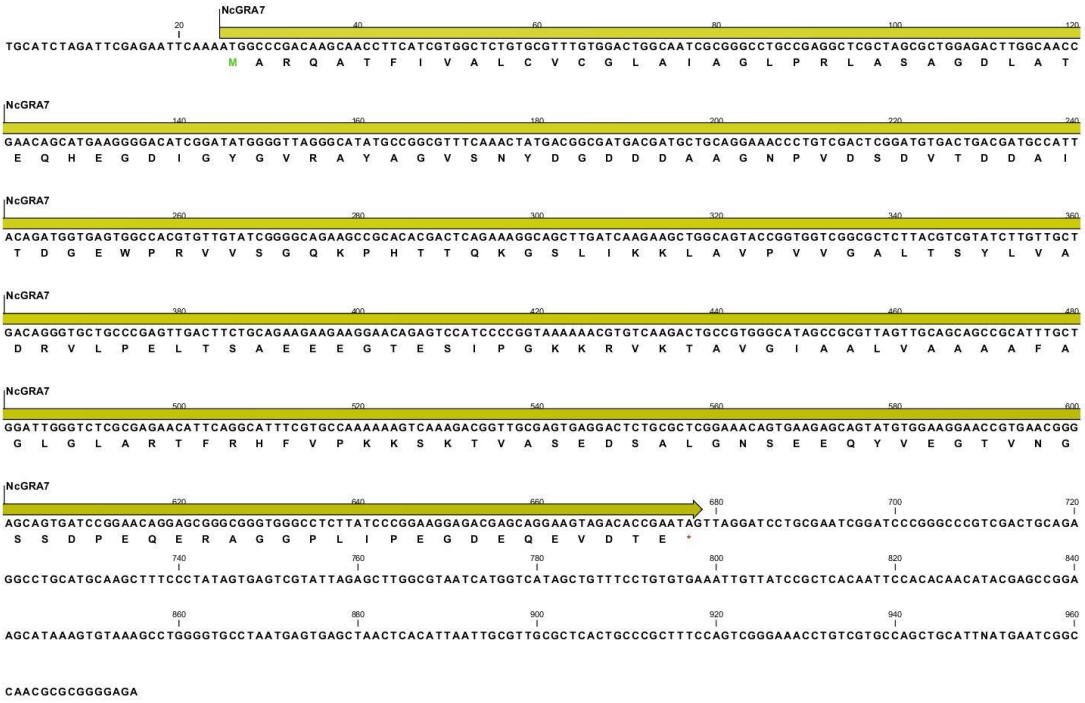

Figure 3. Nucleotide and translated sequence of NcGRA7.

identity with other recorded NcGRA7 genes in genebank. Similarity of this gene with Toxoplasma gondii GRA7 genes varied between 34-45%.Various physico-chemical properties of studied protein were computed using ProtParam program. ProtParam analysis results are shown in Table 1.

Table 1. Physico-chemical properties of NcGRA7 protein derived from ProtParam.

Number of amino acids	217
Molecular weight	22494.9
Theoretical pI	4.54
Negatively charged residues (Asp + Glu)	34
Positively charged residues (Arg + Lys)	19
Formula	C 977 H 1562 N 272 O 330 S 3
Total number of atoms	3144
Extinction coefficients	13075 (12950)
Estimated half-life	30 hours (mammalian reticulocytes, in vitro) >20 hours (yeast, in vivo) >10 hours (Escherichia coli, in vivo)
Instability index	29.87
Aliphatic index	84.56
GRAVY	-0.216

Discussion

In this study, UV spectrophotometry was used in order to take advantage of this method one needs an accurate measure of the protein of interest's extinction coefficient (molar absorption coefficient). The extinction coefficient indicates how much light a protein absorbs at a certain wavelength. This estimation is useful for following a protein with a spectrophotometer when purifying it. Two values are produced by ProtParam, both for proteins measured in water at 280 nm. The first one shows the computed value based on the assumption that all cysteine residues appear as half cystines (i.e. all pairs of Cys residues form cystines), and the second one assuming that no cysteine appears as half cystine (i.e. assuming all Cys residues are reduced). This measure is estimated using the method of Pace et al., which calculates the sum of (NumberAA x Extinction Coefficient AA) for three amino acids that absorb at 280 nm: tyrosine, tryptophan, and the dimeric amino acid cystine (two cysteine [Cys] residues covalently joined through a disulfide bond. The absorbance of the protein at 280 nm (A280, or OD280) is calculated by dividing the extinction coefficient by the molecular weight of the protein.

The half-life is a prediction of the time it takes for half of the amount of protein in a cell to disappear after its synthesis in the cell. ProtParam relies on the "N-end rule", which relates the half-life of a protein to the identity of its N-terminal residue; the prediction is given for 3 model organisms (human, yeast and E. coli). The N-end rule states that the in vivo half-life of a protein is a function of the nature of its amino-terminal residue (Bachmair et al., 1986). Because the N terminus amino acid of NcGRA7 protein is Methionine, so based on N-end rule, it will be stable more than 10 hours in E. coli cells.

The instability index provides an estimate of the stability of protein of interest in a test tube. Values greater than 40 indicate that the protein may be unstable in vitro. This index assigns a weighted instability value to each dipeptide in the protein (Guruprasad et al., 1990). These values were derived from an analysis that found a significant difference in the occurrence of certain dipeptides between stable and unstable proteins. Analysis by ProtParam revealed that NcGRA7 can be classified as a stable protein (Instability index: 29.87).

The protein aliphatic index is defined as the relative volume occupied by aliphatic side chains (alanine, valine, isoleucine, and leucine). It may be regarded as a positive factor for the increase of thermo stability of globular proteins. Aliphatic index is calculated using the method of Ikai as the sum of (Molar %AA x Volume AA) for alanine, leucine, isoleucine and valine (where Volume AA is the relative value compared to alanine). Aliphatic index analysis results was consistent with previously described results from instability index while aliphatic index is defined as a measure of thermostability, lower value of instability index for NcGRA7 can be contributed to aliphatic index. In other words, higher aliphatic index is related to lower instability index and higher stability.

A GRAVY (Grand Average of hydropathicity) score can be calculated as the sum of the hydropathy values for all the amino acids in a protein sequence divided by the number of residues in the sequence. In essence, a GRAVY score is the relative value for the hydrophobic residues of the protein. Although no positional or interaction effects for adjacent residues are taken into consideration by the GRAVY score, it still provides some indication of the physical state of the protein

(Kyte and Doolittle, 1982).

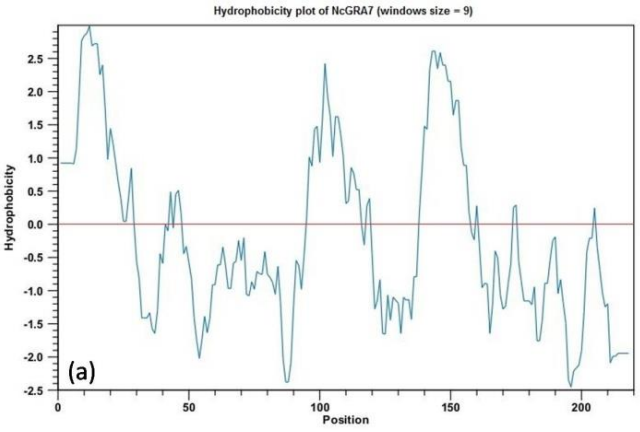

Figure 4. Hydrophobicity plots of the NcGRA7 (a) windows size = 9

This index indicates the solubility of the proteins: positive GRAVY protein is hydrophobic while negative GRAVY protein is hydrophilic (Kyte and Doolittle, 1982). As derived from ProtParam analysis, NcGRA7 gained a negative GRAVY score so it can be inferred that NcGRA7 is a hydrophilic protein. According to Kyte and Doolittle (1982), integral membrane proteins typically have higher GRAVY scores than do globular proteins. Though this score is another helpful piece of information, it cannot reliably predict the structure without the help of hydropathy plots.

There are some methods for evaluation of the degree of interaction of polar solvents such as water with specific amino acids. In these methods a hydrophobicity plot is created that is a quantitative analysis of the degree of hydrophobicity or hydrophilicity of amino acids in a protein (Kyte-Doolittle scale indicates hydrophobic amino acids, while the Hopp-Woods scale measures hydrophilic residues). This measure is implicated to identify possible structure or domains of a protein. Plot shape analysis prepares information about partial structure of the protein of interest. For example, extension of about 20 amino acids with positive shows that these amino acids may be part of alpha-helix spanning across a lipid bilayer, which is composed of hydrophobic fatty acids. On the other hand, stretch of amino acids with negative hydrophobicity indicates that these residues are in contact with solvent or water, and that they are probably resided on the outer surface of the protein. To elucidate properties of NcGRA7, the hydrophobicity plot of the deduced protein sequence was reproduced based on Kyte and Doolitlle (1982) algorithm (Fig 4). Two plots were drawn for NsGRA7; one of them was plotted with windows size of 9 for seeking surface regions and second one was plotted with windows size of 19 to look for transmembrane regions. As shown in Figure 4-a, possible surface regions can be identified as strong negative peaks. In Figure 4-b, transmembrane regions are identified by peaks with scores greater than 1.6.

Protein signature databases are essential tools to identify relationships between sequences, so they can be implicated for protein classification and inferring their function. InterProScan (Zdobnov and Apweiler, 2001) is a tool that combines different protein signature recognition methods into one resource. InterProScan results were summarized in Fig. 5 and Table 2.

Figure 5. InterProScan visual output for NcGRA7.

Table 2. NcGRA7 confidently predicted domains and features.

Name	Begin	End
signal peptide	1	27
transmembrane	138	160

As mentioned earlier, dense granule antigens (GRAs) are secreted from the *N. caninum* tachyzoite. Gra7 is released by the parasite during intra-vacuolar habitation. NcGRA7 is a 5-element fingerprint that provides a signature for the dense granule Gra7 proteins. The fingerprint was derived from an initial alignment of 2 sequences: motif 1 lies in the putative signal sequence and motif 4 encodes the putative transmembrane domain (Table 2).

Jukes-Cantor distance between each pairs of sequences was calculated (Fig. 6 – upper diagonal). This number is given as the Jukes-Cantor correction of the proportion between identical and overlapping

alignment positions between the two sequences. Also Percent identity calculated as the percentage of identical residues in alignment positions to overlapping alignment positions between each pair of sequences (Fig. 6 – lower diagonal).

		1	2	3	4	5
AF176649	1		0.02	0.02	0.28	0.48
NCU72991	2	98.50		0.01	0.27	0.47
NCU82229	3	98.00	98.83		0.26	0.46
NCU36386	4	76.37	77.05	77.82		0.36
NcGRA7 (Current Study)	5	64.55	64.97	65.73	71.18	

Figure 6. Upper diagonal: Calculated pairwise Jukes-Cantor distance, Lower diagonal: Calculated pairwise percent identities.

To determine the phylogenetic position of the NcGRA7 in the current study, its sequence was used for comparative sequence analysis against known NcGRA7 sequences. The NcGRA7 sequence of the current study showed a high relationship to each of known sequences of the NcGRA7 (Fig. 7).

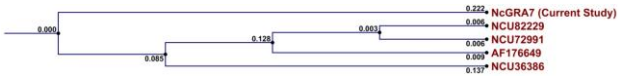

Figure 7: Phylogeny of NcGRA7 sequence of the current study. The tree was constructed using the UPGMA method. Numbers along branches represent length values.

N. caninum is an obligatory intracellular parasite which has complicated life cycle and almost infects all nucleated cells (Dubey and Schares, 2011). *N. caninum* causes dangerous manifestation in fetus which the most dangerous effect of congenital neosporosis is abortion (Dubey and Schares, 2011; Sadrebazzaz et al., 2004). The congenital infection has different symptoms based on the intensity and variety of contamination in the organs. Severity of the disease is related to stage of the pregnancy period which the infection occurs (Salehi et al., 2009). In this study, the NcGRA7 gene of *Neospora caninum* tachyzoites surface antigen was cloned for studying its immunogenic potentials in future. In conclusion, a 679 bp length fragment of a gene corresponding to the 22 kDa protein gene of *Neospora caninum* tachyzoites dense granule protein (NcGRA7) was cloned and verified by sequencing and bioinformatics analysis and expression of this gene is the next step to prepare an effective vaccine formula against neosporosis.

Acknowledgements

The authors thank the Institute of Biotechnology, Ferdowsi University of Mashhad for financial support of this study (grant no. 100040) and the directors of the Razi vaccine and serum research institute, Mashhad branch and animal biotechnology lab in department of animal sciences, college of agriculture, Ferdowsi University of Mashhad, in which this study was performed.

References

1- Augustine P. C., Jenkins M. C. and Dubey J. P. (1999) Effect of polyclonal antisera developed against dense granule-associated Neospora caninum proteins on cell invasion and development in vitro by N. caninum tachyzoites. Parasitology 119 (Pt 5):441-445.

2- Bachmair A., Finley D. and Varshavsky A. (1986) In vivo half-life of a protein is a function of its amino-terminal residue. Science 234:179.

3- Bjerkas I. and Presthus J. (1988) Immuno-histochemical and ultrastructural characteristics of a cyst-forming sporozoon associated with encephalomyelitis and myositis in dogs. APMIS 96:445-454.

4- Cesbron-delauw M. F. (1994) Dense granule organelles of Toxoplasma gondii : the role in the host-parasite relationship. Parasitol Today 10:239-246.

5- Cho J. H., Chung W. S., Song K. J., Na B. K., Kang S. W., Song C. Y. and Kim T. S. (2005) Protective efficacy of vaccination with Neospora caninum multiple recombinant antigens against experimental Neospora caninum infection. Korean J Parasitol 43:19-25.

6- Dubey J. P., Carpenter J. L., Speer C. A., Topper M. J. and Uggla A. (1988) Newly recognized fatal protozoan disease of dogs. J Am Vet Med Assoc 192:1269-1285.

7- Dubey J. P. and Schares G. (2011) Neosporosis in animals - the last five years. Vet Parasitol 180:90-108.

8- Guruprasad K., Reddy B. V. B. and Pandit M. W. (1990) Correlation between stability of a protein and its dipeptide composition: a novel approach for predicting in vivo stability of a protein from its primary sequence. Protein Eng 4:155-161.

9- Haddadzadeh H. R., Sadrebazzaz A., Malmasi A., Talei Ardakani H., Khazraii Nia P. and Sadreshirazi N. (2007) Seroprevalence of Neospora caninum infection in dogs from rural and urban environments in Tehran, Iran. Parasitol Res 101:1563-1565.
10- Hopp T. P. and Woods K. R. (1981) Prediction of protein antigenic determinants from amino acid sequences. Proceedings of the National Academy of Sciences 78:3824.
11- Hosseininejad M., Hosseini F., Mahzounieh M., Raisi Nafchi A. and Mosharraf M. (2010) Seroprevalence of Neospora caninum infection in dogs in Chaharmahal-va-Bakhtiari Province, Iran. Comp Clin Pathol 19:269-270.
12- Hosseininejad M., Pirali-Kheirabadi K. and Hosseini F. (2009) Seroprevalence of Neospora caninum Infection in Camels (Camelus dromedarius) in Isfahan Province, Center of Iran. Iranian J Parasitol 4:61-64.
13- Howe D. K. and Sibley L. D. (1999) Comparison of the major antigens of Neospora caninum and Toxoplasma gondii. Int J Parasitol 29:1489-1496.
14- Huang P., Liao M., Zhang H., Lee E. G., Nishikawa Y. and Xuan X. (2007) Dense-granule protein NcGRA7, a new marker for the serodiagnosis of Neospora caninum infection in aborting cows. Clin Vaccine Immunol 14:1640-1643.
15- Jenkins M., Parker C., Tuo W., Vinyard B. and Dubey J. P. (2004) Inclusion of CpG adjuvant with plasmid DNA coding for NcGRA7 improves protection against congenital neosporosis. Infect. Immun. 72:1817-1819.
16- Kyte J. and Doolittle R. F. (1982) A simple method for displaying the hydropathic character of a protein. J Mol Biol 157:105-132.
17- Lally N., Jenkins M., Liddell S. and Dubey J. P. (1997) A dense granule protein (NCDG1) gene from Neospora caninum. Mol Biochem Parasitol 87:239-243.
18- Larkin M., Blackshields G., Brown N., Chenna R., McGettigan P., McWilliam H., Valentin F., Wallace I., Wilm A. and Lopez R. (2007) Clustal W and Clustal X version 2.0. Bioinformatics 23:2947-2948.
19- Liddell S., Parker C., Vinyard B., Jenkins M. and Dubey J. P. (2003) Immunization of mice with plasmid DNA coding for NcGRA7 or NcsHSP33 confers partial protection against vertical transmission of Neospora caninum. J Parasitol 89:496-500.
20- Malmasi A., Hosseininejad M., Haddadzadeh H., Badii A. and Bahonar A. (2007) Serologic study of anti-Neospora caninum antibodies in household dogs and dogs living in dairy and beef cattle farms in Tehran, Iran. Parasitol Res 100:1143-1145.
21- Monney T., Debache K. and Hemphill A. (2011) Vaccines against a Major Cause of Abortion in Cattle, Neospora caninum Infection. Animals 1:306-325.
22- Nematollahi A., Jaafari R. and Moghaddam G. (2011) Seroprevalence of Neospora caninum Infection in Dairy Cattle in Tabriz, Northwest Iran. Iran J Parasitol 6:95-98.
23- Nishikawa Y., Zhang H., Ikehara Y., Kojima N., Xuan X. and Yokoyama N. (2009) Immunization with oligomannose-coated liposome-entrapped dense granule protein 7 protects dams and offspring from Neospora caninum infection in mice. Clin Vaccine Immunol 16:792-797.
24- Nourollahi Fard S. R., Khalili M. and Aminzadeh A. (2008) Prevalence of antibodies to Neospora caninum in cattle in Kerman province, South East Iran. Vet Arh 78:253.
25- Petersen T. N., Brunak S., von Heijne G. and Nielsen H. (2011) SignalP 4.0: discriminating signal peptides from transmembrane regions. Nat. Methods 8:785-786.
26- Razmi G. R., Mohammadi G. R., Garrosi T., Farzaneh N., Fallah A. H. and Maleki M. (2006) Seroepidemiology of Neospora caninum infection in dairy cattle herds in Mashhad area, Iran. Vet Parasitol 135:187-189.
27- Sadrebazzaz A., Habibi G., Haddadzadeh H. and Ashrafi J. (2007) Evaluation of bovine abortion associated with Neospora caninum by different diagnostic techniques in Mashhad, Iran. Parasitol Res 100:1257-1260.
28- Sadrebazzaz A., Haddadzadeh H., Esmailnia K., Habibi G., Vojgani M. and Hashemifesharaki R. (2004) Serological prevalence of Neospora caninum in healthy and aborted dairy cattle in Mashhad, Iran. Vet Parasitol 124:201-204.
29- Sadrebazzaz A., Haddadzadeh H. and Shayan P. (2006) Seroprevalence of Neospora caninum and Toxoplasma gondii in camels (Camelus dromedarius) in Mashhad, Iran. Parasitol Res 98:600-601.
30- Salehi N., Haddadzadeh H., Ashrafihelan J., Shayan P. and Sadrebazzaz A. (2009) Molecular and Pathological Study of Bovine Aborted Fetuses and Placenta from Neospora caninum Infected Dairy Cattle. Iran J Parasitol 4:40-51.
31- Sambrook J., Fritsch E. F. and Maniatis T. 1989. Molecular cloning: a laboratory manual. New York: Cold Spring Harbor Laboratory Press.
32- Sigrist C. J. A., Cerutti L., De Castro E., Langendijk-Genevaux P. S., Bulliard V., Bairoch A. and Hulo N. (2010) PROSITE, a protein domain

database for functional characterization and annotation. Nucleic Acids Res 38:D161-D166.
33- Soltani M., Sadrebazzaz A., Nassiri M. and Tahmoorespoor M. (2013) Cloning, Nucleotide Sequencing and Bioinformatics Study of NcSRS2 Gene, an Immunogen from Iranian Isolate of Neospora caninum. Iranian journal of parasitology 8:114.
34- Vonlaufen N., Guetg N., Naguleswaran A., Muller N., Bjorkman C., Schares G., von Blumroeder D., Ellis J. and Hemphill A. (2004) In vitro induction of Neospora caninum bradyzoites in vero cells reveals differential antigen expression, localization, and host-cell recognition of tachyzoites and bradyzoites. Infect. Immun. 72:576-583.
35- Yagoob G. (2011) Seroprevalence of Neospora Caninum in Stray Dogs. Am J Anim Vet Sci 6:100-104.
36- Zdobnov E. M. and Apweiler R. (2001) InterProScan–an integration platform for the signature-recognition methods in InterPro. Bioinformatics 17:847-848.

Cytogenetic study of two *Solenanthus* Ledeb. species (Boraginaceae) in Iran

Massoud Ranjbar, Maryam Almasi and Elnaz Hosseini

Department of Biology, Herbarium division, Bu-Ali Sina University, P. O. Box 65175/4161, Hamedan, Iran

Received 25 July 2013 Accepted 01 September 2013

Abstract

Chromosome number, meiotic behavior, and pollen viability were analyzed in 2 species of *genus Solenanthus*, *S. stamineus* (Desf.) Wettst. and *S. circinnatus* Ledeb, from Iran. This report is the first cytogenetic analysis of these species. All taxa are diploid and possess $2n = 2x = 24$ chromosome number, consistent with the proposed base number of $x = 12$. Although this taxon displayed regular bivalent pairing and chromosome segregation at meiosis, but some abnormalities were observed.

***Keywords*:** Boraginaceae, chromosome number, meiotic behavior, pollen viability, *Solenanthus*.

Introduction

The family Boraginaceae consists of 156 genera distributed throughout the tropical, subtropical and temperate regions (Al-Shehbaz, 1991; Ge-Ling, 1995). The genus *Solenanthus* belongs to tribe Cynoglosseae DC. and is mainly distributed in the north temperate regions, but centers of diversity are in the eastern Mediterranean area and western Asia (Al-Shehbaz, 1991). Morphologically, the genus is characterized by tubular corollas, long or short anthers, a style often exerted from the corolla. Nutlets dorsiventrally compressed, with dense glochids on abaxial margin (Riedl, 1967).

Materials and Methods

Cytogenetic

The chromosome number and meiotic behavior were analyzed in one population of *Solenanthus stamineus* and two populations of *S. circinnatus* which were collected from different regions within the natural geographical distribution of them during several excursions in Iran (table1). Fifteen flower buds at an appropriate stage of development were fixed in 96% ethanol, chloroform and propionic acid (6:3:2) for 24 h at room temperature and then stored in 70% ethanol at 4 °C until used. Anthers were squashed and stained with 2% acetocarmine. All observations were photographed using an Olympus 3030 digital camera mounted on a BX-51 Olympus microscope.

∗Corresponding author E-mail: *ranjbar80@yahoo.com*

Pollen viability

Pollen stainability was considered as an indication of pollen viability. For this purpose pollen grains were first obtained from the flowers of herbarium specimen and then stained with acetocarmin/glycerin (1:1). Slides were stored at room temperature for 24-48 hours. The stainability was determined using samples of 1000 pollen grains per flower. Slides were examined and documented with an Olympus BX-51 photomicroscope.

Taxa	Herbarium number	Altitude (m)	Location	Date	Collector
S. circinnatus	35067	2144	Chaharmahal-e Bakhtiari, Gandoman toward Yasuj, Cheshmeh-Ali area	27.4.2011	Ranjbar & Almasi
S. circinnatus	33047	3700	Kohgiluyeh va Boyer-Ahmad, Eastern Dena, Gol mountain	28.4.2011	Ranjbar & Almasi
S. stamineus	35067	2250	Isfahan, Semirom, protected area of Hana	28.4.2012	Ranjbar & Almasi

Results

Chromosome number and meiotic behavior

All species analyzed by mitotic chromosome counting had a consistent number of $n = 12$ in pollen mother cells (PMCs). All taxa studied here displayed regular bivalent pairing and chromosome segregation at meiosis. However, some meiotic

abnormalities were observed. The meiotic irregularities observed

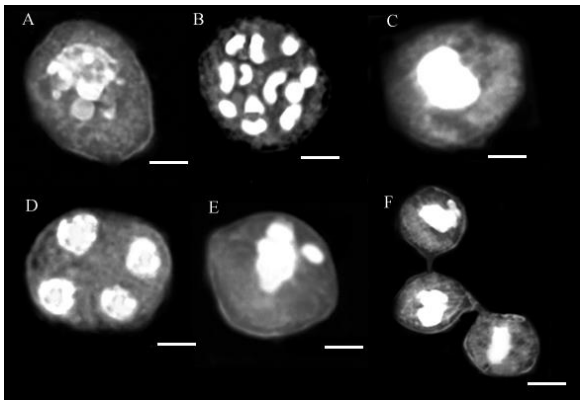

Figure 1. Representative meiotic cells in *S. circinnatus* 44 with *n* = 12. (A) Porophase, (B) Diakinesis, (C) Metaphase I, (D) telophase II, (E) Precocious migration to poles (F) Cytomixis in metaphase I. Scale bar = 3 μm.

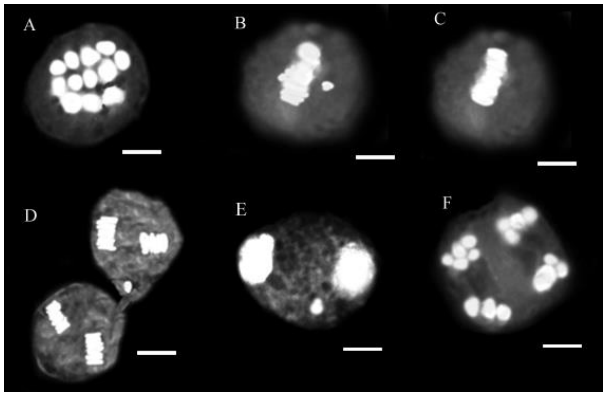

Figure 2. Representative meiotic cells in *S. circinnatus* 47 with n = 12. (A) Diakinesis, (B) Precocious migration to poles in metaphase I, (C) Metaphase I, (D) Cytomixis in telophase II, (E) Micronucleus in telophase I, (F) Anaphase II. Scale bar = 3 μm.

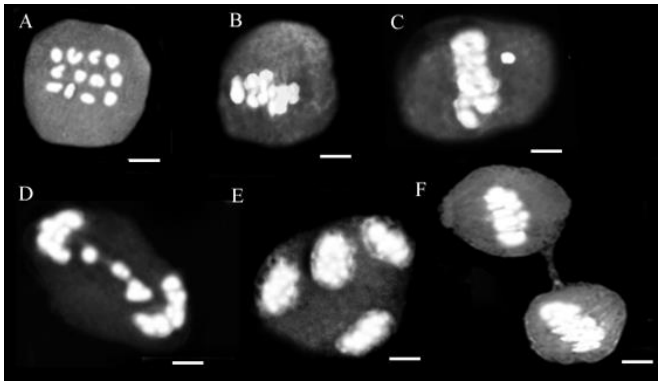

Figure 2. Representative meiotic cells in *S. stamineus* with *n* = 12. (A) Diakinesis, (B) Metaphase I, (C) Precocious migration to poles in metaphase I, (D) Laggard chromosome in Anaphase I, (E) Telophase I, (F) Cytomixis in metaphase I. Scale bar = 3 μm.

in different *Solenanthus* species included the occurrence of varied degree of precocious migration to poles, cytomixis and laggard chromosomes (table 2 and figures 1-3).

Cytomixis

The observation of cytomixis in metaphase I and telophase II stages of meiosis was one of irregularity in the studied genotypes. The phenomenon of cytomixis is characterized by the migration of chromatin/chromosomes between the proximate meiocytes through cytoplasmic channels or intercellular bridges. Though an infrequent cytological phenomenon, it has been reported to occur in a large array of plant species (Gottschalk, 1970; Cheng et al., 1975; Omara, 1976; Guochang, et al., 1987; Bedi et al., 1990; Bellucci et al., 2003). Cytoplasmic connections preexist between meiocytes in the form of plasmodesmata within the syncytium and then become severed as a result of insulation of meiocytes by the progressive deposition of callose (Heslop-Harrison, 1966). In some cases, however, the plasmodesmata still persist during meiosis and increase in size to generate cytomictic connections. These are termed as cytomictic channels and are large enough to permit the transfer of cytoplasmic organelle and in some cases chromatin material (Risueno et al, 1969; Lattoo et al., 2006; Ranjbar et al., 2011a).

Precocious migration to the poles and laggard chromosome

The most frequent abnormalities in the two meiotic divisions were those related to chromosome segregation, such as precocious migration to the poles during metaphase and laggards at anaphase (figure 1-3) that led to the formation of micronuclei at telophase. However, in this accession, only a few cells with micronuclei (1.7%) were detected in telophase I.

Micronucleus

Micronucleus is another abnormality that was found in *S. circinnatus* 47 (figure 2.) Chromosomes that produced micronuclei during meiosis were eliminated from microspores as microcytes. The micronucleus reached the microspore wall and formed a kind of bud, separated from the microspore. The eliminated microcytes gave origin to small and sterile pollen grains (Baptists-Giacomoelli et al., 2000; Ranjbar et al., 2009, 2010, 2011b).

Pollen viability

The results of the comparison between meiotic behavior and pollen viability showed the highest (99) and lowest (94) percentages of the stained pollens in *S. stamineus* and *S. circinnatus* 44, respectively. This result indicates that irregularities observed at meiosis probably have a direct relation with species fertility. The pollen viability of examined species are described in table 2 and illustrated in figure 4.

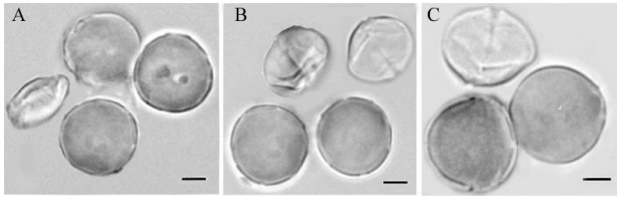

Figure 4. Pollen viability. (A) *S. stamineus*, (B) *S. circinnatus* 47, (C) *S. circinnatus* 44. Scale bar = 2 μm.

Table2. Characterization of meiotic behaviour and Pollen viability in one population of *S. stamineus* and two populations of *S. circinnatus* .

Meiotic characters	*S. circinnatus*	*S. circinnatus* 44	*S. circinnatus* 47
Cell number	480	431	290
D/MI	50	290	120
% D/MI	10	67	41
% Cytomixis	2	0	5
% Precocious migration to poles	3	8	6
AI/TI	220	65	10
% AI/TI	46	15	3.5
% Laggard chromosome	0	1	2
MII	80	0	20
% MII	16	0	7
AII/TII	130	76	140
% AII/TII	27	18	48
% Cytomixis	0	1	3
% micronucleus			1.7
% Laggard chromosome	0	0	2
x	12	12	12
% Pollen viability	99	98	94

Discussion

The most common chromosome number in tribe Cynoglosseae is $n = 12$ and has the lowest variation in contrast with the other tribes (Britton, 1951; Coppi et al., 2006).

Besides these, Coppi et al. (2006) also found evolution of new forms in this tribe seem to have involved minor chromosomal rearrangements with respect to tribe Boragineae and Lithospermeae, also in terms of changes in ploidy levels. There is a considerable difference in the size of the chromosomes between the genera of tribe Cynoglosseae (Britton, 1951). The relatively high base number $x = 12$ is possibly derived from lower ones in other tribes, such as $x = 6$ and this may support the traditional view that Cynoglosseae represent "the most highly specialized tribe in the family" (Johnston, 1924; Britton, 1951).

The present work confirmed that both species of *Solenanthus* are diploid with $2n = 2x = 24$ chromosomes, as reported in the literature. The meiosis is regular, with normal chromosome pairing, possibly existing chromosomes with complete and/or incomplete pairing. Many abnormalities were observed during the meiosis, as sticky chromosomes and irregular chromosome segregation.

According to Hartl and Jones (1998), mitotic and meiotic divisions in eukaryotic cells are rigorously controlled by checkpoint mechanisms intending to preserve the genome integrity. When at least one single chromosome does not present spindle fibers attached to the kinetochore during the metaphase, or when it is not aligned along the metaphase plate, specific proteins from the kinetochore signalize to delay the cellular division until the normal situation would be restored by proteins that act to maintain the genomic integrity during the cell cycle. Thus, proteins that control the repair mechanism during metaphase I and II could have been activated by the kinetochores of the delayed chromosomes, obstructing the elimination of those delayed chromosomes and the later formation of micronuclei have been observed in *S. circinnatus* 47.

The highest percentage of stained pollen grain (99%) was recorded for *S. stamineus*. This result is predictable based on meiotic behavior data and of the lowest percentages of irregularities in this population (table 2). In contrast, a lower percentage of pollen viability (94%) in population of *S. circinnatus* 47 can be explained by having high percent of precocious migration to the poles during metaphase and laggards at anaphase that led to the formation of micronuclei at telophase and could be provide small and sterile pollen grains.

Acknowledgment

The authors would like to thank the Bu-Ali Sina University for the financial support.

References

1- Al-shahbaz I. (1991) the genera of Boraginaceae in the southeastern united states. Journal of the Arnold Arboretum 1: 1-169.
2- Baptists-Giacomelli F. R., Pagliarini M. S. and Almeida J. L. (2000) Elimination of

micronuclei from microspores in a Brazilian oat (*Avena sativa* L.) variety. Genetic Molecular of Biology 23: 681-684.

3- Bedi Y. S. (1990) Cytomixis in woody species. Proceedings of the Indian Academy of Science (Plant Science.) 100: 233-238.

4- Bellucci M., Roscini C. and Mariani A. (2003) Cytomixis in pollen mother cells of *Medicago sativa* L. Journal of Heredity 94: 512-516.

5- Britton D. M. (1951) Cytogenetis studies on the Boraginaceae. Brittonia 7: 233-266.

6- Cheng K. C., Nieh H. W., Yang C. L., Wang I. M., Chou I. S. and Chen J. S. (1975) Light and electron microscopial observations on cytomixis and the study of its relation to evolution. Acta Botanica Sinica 17: 60-69.

7- Coppi A., Selvi F. and Bigazzi M. (2006) Chromosome studies in Mediterranean species of Boraginaceae. Flora Mediterranea 16: 253-274.

8- Ge-ling z., Riedl h. and kamelin h. (1995) Boraginaceae. In: Zhengyi W.and Raven P. H. eds., Flora of China, vol. 16. St Louis and Beijing, Missouri Botanical Garden Press.

9- Gottschalk W. (1970) Chromosome and nucleus migration during microsporogenesis of *Pisum sativum*. Nucleus 13: 1-9.

10- Guochang Z., Quinglan Y. and Yongren Z. (1987) The relationship between cytomixis, chromosome mutation and karyotype evolution in lily. Caryologia 40: 243-259.

11- Hartl D. L. and Jones E. W. (1998) Genetics: Principles and analyses. 4th edition. Jones and Bartlett Publishers, Sudbury, Massachusets.

12- Heslop-Harrison J. (1966) Cytoplasmic connection between angiosperm meiocytes. Annals of Botany. 30: 221-230.

13- Lattoo S. K., Khan S., Bamotra S. and Dhar A. K. (2006) Cytomixis impairs meiosis and influences reproductive success in *Chlorophytum comosum* (Thunb) Jacq. - an additional strategy and possible implications. Journal of Biosciences. 31: 629-637.

14- Omara M. K. (1976) Cytomixis in *Lolium perenne*. Chromosoma 55: 267-271.

15- Ranjbar M., Karamian R. and Hadadi A. (2009) Biosystematic study of *Onobrychis vicifolia* Scop. And *Onobrychis altissima* Grossh. (Fabaceae) in Iran. Iranian Journal of Botany 15 (1): 85-95.

16- Ranjbar M., Karamian R. and Hajmoradi F. (2010) Chromosome number and meiotic behaviour of two populations of *Onobrychis chorassanica* Bunge (O. sect. *Hymenobrychis*) in Iran. Journal of Cell and Molecular Research 2: 49-55.

17- Ranjbar M., Karamian R. and Hajmoradi Z. (2011a) Cytomorphological study of *Trigonella disperma* (Fabaceae) in Iran. Cytologia 76 (3): 279-294.

18- Ranjbar M., Hajmoradi Z. and Karamian R. (2011b) Cytogenetic study and pollen viability of four populations of *Trigonella spruneriana* Boiss. (Fabaceae) in Iran. Journal of Cell and Molecular Research 3: 19-24.

19- Riedel H. 1967 Boraginaceae. In: Rechinger K. H. ed., Flora Iranica, vol. 48. Akademische Druck- und Verlagsanstalt, Graz.

20- Risueno M. C., Gimenez-Martin G., Lopez-Saez J. F. and R-Garcia M. I. (1969) Connexions between meiocytes in plants. Cytologia 34: 262-272.

Medium optimization for biotechnological production of single cell oil using *Yarrowia lipolytica* M_7 and *Candida* sp.

Marjan Enshaeieh*, Azadeh Abdoli, and Iraj Nahvi

1. Department of Biology, Falavarjan branch, Islamic Azad University, Esfahan, Iran
2. Department of Biology, Esfahan University, Esfahan, Iran

Received 01 August 2013 Accepted 14 September 2013

Abstract

Microbial lipids have a great similarity to the lipids obtained from plants and animals. Triacylglycerol is the storage lipid in most of eukaryotic cells; this characteristic attracts a lot of attention for using these lipid sources in biodiesel production. Accumulation of neutral lipid composed of triacylglycerol and sterylster is an induced response to environmental stresses in many living organisms. In this situation lipid accumulates as intracellular lipid bodies in yeast cells. Production of microbial oil has more cost than plant's oil. In this case, reducing the cost of this process must be done by optimization of culture conditions to reach higher production yield. In this study the effect of physical parameters on lipid production of two oleaginous yeasts: *Yarrowia lipolytica* M7 and *Candida sp.* was investigated. The mentioned parameters were pH range of 4-7; centrifugation rates of 100, 150, 200 rpm; temperature of 15, 25, 35 and 45ºC and times of incubation of 24, 48, 72 and 96 h. Temperature and time of incubation had a significant effect on lipid production by these strains and optimization of them resulted in increased production of lipid from 25% to 34% in *Yarrowia lipolytica* M7.

Keywords: physical parameters, oleaginous yeasts, *Yarrowia lipolytica* M_7

Introduction

Eukaryotic cells can accumulate lipid in intracellular lipid bodies. The structure of these lipid droplets is similar in all eukaryotic cells with a hydrophobic nucleus and a phospholipid layer around it (Drucken, 2008; Mullner and Duam, 2004; Melickova et al., 2004). The similarity of the lipid accumulated in microorganisms such as molds and yeasts is very important because it can be used as the substrate for biodiesel production and many other industrial purposes. Yeasts cells that can accumulate lipid more than 20% of their biomass are called as oleaginous yeasts (Meng et al., 2009; Liu et al., 2010). Among oleaginous yeasts less than 5% of them can accumulate more than 25% of lipid (Manuel et al., 2011). Two important enzymes i.e. malic enzyme and ATP-citrate lyase are involved in lipid accumulation process. There is a great relationship between ATP-citrate lyase activity and potential of lipid accumulation in yeasts cells (Meng et al., 2009; Fidler et al., 1999; Fei et al., 2008). Lipid body formation starts at the end of exponential phase and continues during stationary phase (Raschke and Knorr, 2009). When nitrogen limited condition occurs, nicotine amid adenine dinucleotide isocitrate dehydrogenase activity reduced and affect the tricarboxilic acid cycle, change the metabolism pathway and interrupt protein synthesis, resulting in the activation of lipid accumulation process (Pan et al., 2009; Wynn and Ratledge, 2005). Beyond nitrogen limitation, phosphate limitation can also improve lipid accumulation in oleaginous microorganisms (Muniraj et al., 2013).

Oleaginous micro-organisms attract a lot of attention because of their high growth rate and ability to use different carbon sources (Economou et al., 2011; Liu et al., 2010). Also they have short life cycle and are resistant against climatic and seasonal changes, so they have good advantages over plants, being used as oil producing organisms (Li et al., 2008; Amaretti et al., 2008; Zhao et al., 2008). Substituting of microbial lipid instead of plant's oil for biodiesel production is a developing idea (Fakas et al., 2008; Karatay and Donmes, 2010).

Physical parameters such as pH, shaker rpm, time and temperature of incubation can effect on lipid production in oleaginous yeasts (Li et al., 2008). Lipid production decreases remarkably in pH 4 and 8 (Syed et al., 2006). The optimum pH is not only different for various oleaginous yeasts but

*Corresponding author E-mail: *m_enshaeieh@yahoo.com*

also is different for different carbon sources (Angerbauer et al., 2008). About the temperature of incubation, oleaginous yeasts have two groups: the first group has higher lipid production in lower temperature (25-30ºC) and the second group has higher lipid yield when increasing in temperature accrues 35-45ºC. The composition of the lipid also varies in different temperatures (Saxena et al., 2009). Time of incubation and shaker rpm also effect lipid production (Leesing et al., 2011). According to this information about effective parameters on lipid yield of oleaginous yeasts, they need different culturing conditions for optimal lipid production. In this study, the effect of physical parameters such as pH, shaker rpm, temperature and time of incubation on lipid production of *Yarrowia lipolytica* M_7 and *Candida sp.* was investigated. Optimization of these physical parameters cause higher lipid production by the evaluated yeasts and have shown their potential for industrial application. Optimization is an essential step of each industrial process because it can result in higher production under economical cost. The important parameters that determine the cost of microbial oil are the substrate cost, production rate and the ultimate lipid concentration (Meester et al., 1996). For increasing the rate of production and concentration of the product, optimization of culture condition, has great importance. FTIR spectroscopy was used to confirm the composition of produced lipid and the results showed the potential of this lipid in biodiesel production.

Materials and Methods

Preparation of inoculums

The oleaginous yeast colonies were first streaked on to YPD (Yeast Extract Peptone Dextrose agar) plates and incubated for 2 days. After that they were transferred in to 250 ml Erlenmeyer flask containing 50 ml of inoculation medium containing: glucose 15g/L, $(NH_4)_2SO_4$ 5g/L, KH_2PO_4 1g/L, $MgSO_4.7H_2O$ 0.5g/L, and yeast extract 0.5g/L and were grown at 28ºC on a shaker at 180 rpm for 2 days(Pan et al., 2009). *Yarrowia lipolytica* M_7 was isolated previously (Mirbagheri et al., 2012) (GenBank accession number, HM011048) and further studies on this strain was done by our research group. *Candid* sp. was isolated from peanut garden and its potential for lipid production was evaluated. Identification of the strain was not important in this study because the work was focused on higher lipid production by doing optimization process for industrial applications.

Preparation of production medium

5 ml of inoculums was transferred to 45 ml of nitrogen-limited medium containing: glucose 40 g/L, $(NH_4)_2SO_4$ 1 g/L, KH_2PO_4 7 g/L, NaH_2PO_4 2 g/L, $MgSO_4.7H_2O$ 1.5 g/L, yeast extract 1 g/l, $CaCl_2$ 0.15 g/L, $MnSO_4.H_2O$ 0.06 g/L, $ZnSO_4.7H_2O$ 0.02 g/L and $FeCl_3.6H_2O$ 0.15 g/L in 250 ml Erlenmeyer flask and incubated in a rotary shaker at 100 rpm, pH 4 and 28ºC for 48h (Pan et al., 2009; Papanikolaou et al., 2001; Kraisintu et al., 2010). This condition is only a trial one to evaluate the lipid production by FTIR spectroscopy. After this step one factorial method was used for evaluating physical parameters on lipid production. First of all, the pH was optimized by changing pH of the culture from 4 to 5, 6 and 7, keeping the other parameters constant and the same method was applied to optimize all other parameters. In one factorial method experiments must be done step by step and in each step only one parameter is variable. The first column of table 1 and 2 shows the variable factor in each trial conditions.

Table1. Lipid yield (g/L), lipid content (%) and biomass (g/L) of *Candida sp.* in different condition

Cultivation condition	Lipid yield (g/L)	Lipid content (%)	Biomass (g/L)
pH			
4	3.01	21.48	14.01
5	3.58	22.85	15.66
6	**3.73**	**22.90**	**16.28**
7	3.15	23.21	13.57
agitation speed (rpm)			
100	3.72	22.90	16.24
150	3.85	23.50	16.38
200	**4.15**	**24.25**	**17.11**
Temperature (°C)			
15	3.80	23.15	16.41
25	**4.25**	**25.16**	**16.89**
35	3.26	22.28	14.71
45	2.80	21.37	13.10
Time of incubation (h)			
24	4.01	24.28	16.51
48	4.35	26.18	16.61
72	4.72	28.72	16.43
96	**4.85**	**31.15**	**15.56**

Table2. Lipid yield (g/L), lipid content (%) and biomass (g/L) of *Yarrowia lipolytica* M_7.

Cultivation condition	Lipid yield (g/L)	Lipid content (%)	Biomass (g/L)
pH			
4	4.48	25.11	17.84
5	**4.78**	**25.80**	**18.52**
6	4.63	25.95	17.84
7	4.60	25.25	18.21
agitation speed(rpm)			
100	4.52	25.12	17.99
150	4.91	26.25	18.70
200	**5.25**	**27.30**	**19.23**
Temperature(°C)			
15	4.95	26.80	18.47
25	**5.59**	**28.15**	**19.40**
35	5.10	26.10	19.54
45	4.60	25.02	18.38
Time of incubation(h)			
24	5.35	29.14	18.35
48	5.68	32.50	17.67
72	**6.25**	**34.15**	**18.30**
96	5.26	31.52	16.68

Determination of lipid productivity to the dry biomass:

5ml of production cultures were harvested by centrifugation at 6000 rpm for 20 min. harvested biomass was washed twice with 5ml of distilled water and then dried at 80ºC to constant mass. The biomass was determined gravimetrically (El-Fadaly et al., 2009; Sriwongchai et al., 2013). Lipid content was determined by the following equation (Kraisintu et al., 2010).

Lipid content = SCO Weight (g/L) / Cell dry weight (g/L) × 100

Single cell oil extraction

Extraction of lipid was carried out according to Bligh and Dyer with modification (Pan et al., 2009). 40 ml of sample was centrifuged at 6000 rpm for 10 min. After that the yeasts were washed with 40 ml of distilled water. This step was repeated, and then 8 ml of 4 M HCl was added in to the biomass and incubated at 70ºC for 2 h. Then acid hydrolyzed mass was stirred with 16 ml chloroform/methanol mixture (1:1) at room temperature for 3 h. At the end centrifugation was done at 5000 rpm for 5 min at room temperature to separate the aqueous upper phase and organic lower phases. Then the lower phase containing lipid was recovered with Pasteur pipette and evaporated in the vacuum. After that the dry lipid was weighed.

Evaluating of physical parameters

The effect of pH varying from 4 to 7 on lipid production was investigated. The culture was prepared same as the production medium, mentioned in previous sections (in each trial condition only one factor was variable). For example at first, pH is the variable parameter and the others are constant; after optimizing this parameter, the other parameters were also optimized repeating the same procedure. After the optimization of pH, the agitation speed of 100, 150 and 200 rpm was evaluated. Cultivation temperature was varied from 15°C to 25°C and 35°C and also 45°C. At the end, the time of incubation at 24, 48, 72 and 96h was varied to evaluate lipid production at each time.

Single cell oil analysis by FTIR spectroscopy:

One of the techniques that can be used to confirm the composition of a product is FTIR spectroscopy. The basic of this method is creating peaks in a special spectrum based on cm^{-1} unit, so each chemical group has a specific peak at a certain point in determined spectrum. Confirmation of certain oil compounds was determined by FTIR spectroscopy using JASCO FT/IR-6300, Japan device. The range of spectrum analyzed by the device was set from 400cm^{-1} to 4000 cm^{-1}. Triolein was used as control sample for comparing with produced single cell oil.

Results

Table 1 and 2 show the results of lipid extraction for *Candida sp.* and *Yarrowia lipolytica* M_7, respectively. The results showed that lipid content of *Candida sp.* reached from 21.48% to 31.15% by optimizing physical condition. About *Yarrowia lipolytica* M_7 lipid content reached from 25.11% to 34.15%. Among physical parameters, temperature and time of incubation have more effect on growth and lipid content. Optimization of physical parameters as well as chemical factors can increase the lipid yield in oleaginous yeasts.

FTIR spectroscopy results

Microbial lipid graphs have been shown in figure 1. Comparison of two graphs shows significant similarity between extracted oil from oleaginous yeasts and the standard (triolein). Significant peaks were between 1670 to 1820 cm^{-1}, confirmed presentation of carbonyl groups. The peaks between 2850 to 2929 cm^{-1} show methyl groups. All of the

peaks in mentioned points showed that produced oil can be converted to biodiesel (Elumalai et al., 2011; European Standard EN 14078; Lin-Vien et al., 1991). Analyzing and confirming of biodiesel compound as an identification method is in number EN 14078 European standard (European Standard EN 14078). The X axis shows wave number which was set between 400 to 4000 (cm^{-1}) and the Y axis shows the percentage of different chemical groups in the evaluating material.

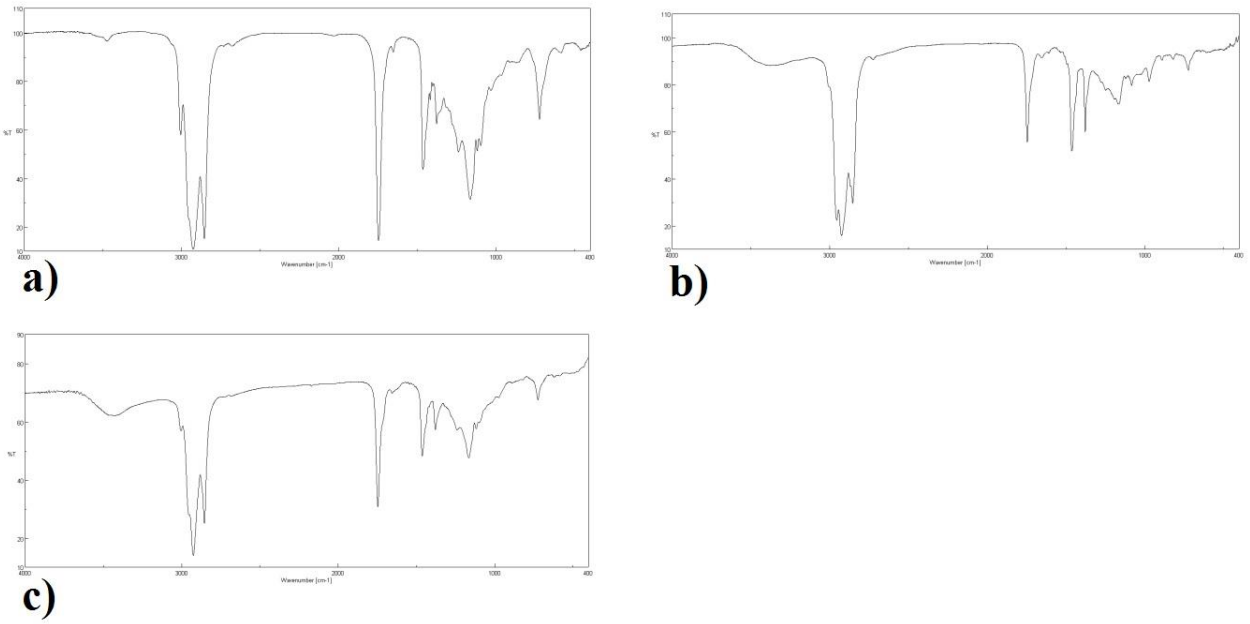

Figure 1: FTIR graphs, (a) FTIR graph of triolein standard, (b) FTIR graph of produced SCO by yeast *Yarrowia lipolytica* M7 (c) FTIR graph of produced SCO by yeast *Candida sp*.

Discussion

Oleaginous yeasts accumulate triacylglycerol rich in unsaturated fatty acids. These lipophylic microbial compounds, because of their special characteristics, are considered from industrial point of view. The first step for application of these oleaginous yeasts in industrial processes is optimization of culture condition. This step cause less time consuming and also less cost is required, so it become valuable from economical point of view. In previous study it was shown that optimization of chemical parameters such as carbon and nitrogen sources, carbon concentration and ammonium concentration can effect on lipid yield in oleaginous yeasts as well as physical parameters (Enshaeieh et al., 2012a). Also the effect of different carbon sources such as glucose, xylose, glycerol and rice bran and different nitrogen sources such as yeast extract, peptone, urea, (NH4)2SO4 and NH4Cl was investigated on lipid production in another study (Enshaeieh et al., 2012 b). Now in this study the optimization process was done by focusing on only the physical parameters.

Leesing et al., in 2011 evaluated lipid production in *Torulaspora globosa* YU5/2 and reported that lipid production decreased after 8 days incubation. Time of incubation for higher lipid production is different among various yeasts. In *Yarrowia sp.* increasing of incubation time, decrease lipid content because they consume the stored lipid after 80 h (papanikolao et al., 2001). Table 2 shows decreasing of about 1 g/L in lipid production of *Yarrowia lipolytica* M7 after increasing of incubation time from 72 h to 96 h. Results showed that by increasing rpm of agitation rate the oxygen that dissolve in the medium become higher and it increase growth and lipid content as metabolisms energy and synthesize of lipid components need oxygen. Accordingly, Oxygen content of the medium has positive relation with lipid accumulation (Liang et al., 2006; Yan et al., 2003; Yi et al., 2006; Tan and Gill, 1985; Choi et al., 1982).

pH of the medium has effect on lipid production by micro-organisms. The influence of pH on lipid production of *Rhodosporidium toruloides* DMKU3-TK16 was investigated by Karisintu et al., in 2010. They found that pH rate of 5.5 was the best one and

lipid production of this strain reach to 9.26 g/L after optimizing other parameters. Angerbauer et al., (2008) reported that in pH rate of 5 the lipid content of lipomyces starky was highest. Acidic and basic condition can affect yeast metabolism because it influence on the enzymes that are evolved in this process and also effect on other components of the yeast cell. For example Johson et al., in 1992 reported that a decrease in ergosterol content of the cell membrane happen as pH increases, so changing in cellular composition with pH seems important for the lipid production in oleaginous yeasts. Limited information about the reason of why pH influences on lipid production is available. The related studies just focus on the effect of pH on optimizing process and did not evaluate the molecular reasons. pH rates of 5-6 is better for higher lipid production in oleaginous yeasts(syed et al., 2006).

El-fadaly et al. in 2009 investigated the effect of incubation time, agitation speed, temperature and pH on lipid production of *Cryptococcus curvatus* NRRLY-1511. The optimized amount of these parameters were 72h, 28ºC, 200 rpm and pH of 5.5, respectively. Syed et al. (2006) showed lipid production decrease in pH rates of 4 and 8. pH of the medium can affect the ability of lipid production and the optimized pH for yeasts cell is between 5 to 6 (Zhu et al., 2008; Easterling et al., 2009; Li et al., 2005).

The results of this investigation showed that by optimization of physical parameters, increase in the lipid production can be done in oleaginous yeasts. By optimizing these factors, the process become more economical than usual and the lipid content of the yeasts become higher. In this investigation lipid content in *Candida sp.* and *Yarrowia lipolytica* M_7 were increased approximately about 10% after optimization. So by optimizing physical parameters higher lipid production and less cost of the process can be obtained.

Acknowledgement

The authors would like to thank Department of Biology of Falavarjan Islamic Azad University for their support of this research work.

References

1- Amaretti A., Raimondi S., Sala M., Roncaglia L., Lucia D. M., Leonardi A. and Rossi M. (2010) Single cell oil of cold adapted oleaginous yeast *Rhodotorula glacialis* DBVPG 4785. Microbial Cell Factoties 23: 59-73.

2- Angerbauer C., Siebenhofer M., Mittelabach M. and Guebitz G. M. (2008) Conversion of sewage sludge in to lipids by *Lipomyces starkeyi* for biodiesel production. Bioresource Technology 99: 3051-3056.

3- Choi S. Y., Ryu Dewey D. Y. and Rhee J. S. (1982) Production of microbial lipid: Effects of growth rate and oxygen on lipid synthesis and fatty acid composition of *Rhodotorula gracilis*. Biotechnology and Bioengineering 24(5): 1165-1172.

4- Drucken Z. (2008) Triacylglycerol synthesis in the oleaginous yeast *Yarrowia lipolytica*. Bioresource Technology 90: 309-319.

5- Easterling E. R., French W. T., Hernandez R. and Licha M. (2009) The effect of glycerol as a sole and secondary substrate on the growth and fatty acid composition of *Rodotorula glutinis*. Bioresource Technology 100: 356-361.

6- Economou C. N., Aggelis G., Pavlou S., Vayenas D. V. (2011) Modeling of single cell oil production under nitrogen-limited and substrate inhibition condition. Biotechnology Bioengineering 108(5): 1049-1055.

7- El-Fadaly H., El-Ahmady N. and Marvan E. M. (2009) Single cell oil production by an oleaginous yeast strain in a low cost cultivation medium. Research Journal of Microbiology 4(8):301-313.

8- Elumalai S., Sakthivel R., Ganesh Kumar S. (2011) Ultra Structural and Analytical Studies of Biodiesel Producing Microalgae (*Chlorella vulgaris* and *Senedesmis* sp.) Collected from Tamil Nadu India. Current Botany 2(6): 19-25.

9- Enshaeieh M., Abdoli A., Nahvi I. and Madani M. (2012) Selection and optimization of single cell oil production from *Rodotorula* 110 using environmental waste as substrate. Journal of cell and molecular research 4(2): 1-10. (a)

10- Enshaeieh M., Abdoli A., Nahvi I. and Madani M. (2012) Bioconversion of different carbon sources in to microbial oil and biodiesel using oleaginous yeasts. Journal of biology and today's world 1(2): 82-92. (b)

11- European Standard EN 14078: Liquid petroleum products –Determination of fatty acid methyl esters (FAME) in middle distillates – Infrared spectroscopy method.

12- Fakas S., Papanikolaou S., Galiotou-Panayotou M., Komaitis M. and Aggelis G. (2008) Biochemistry and biotechnology of Single Cell Oil, Biochemistry and biotechnology of Single Cell Oil. University of Patras 8-60 pp.

13- Fei W., Alfaro G., Muthusamy B. P., Klaassen Z., Graham T. R., Yang H. and Beh C. T. (2008) Genome-wide analysis of sterol-lipid storage and trafficking in *Saccharomyces cerevisiae*, Eukaryotic Cell 7(2): 401-414.
14- Fidler N., Koletzho B. and Sauerwald T. U. (1999) Single cell oil production and application, Pregledni znanstveni prispevek 74 (2): 37-45.
15- Johnson V., Singh M., Saini V. S., Sista V. R. and Yadav N. K. (1992) Effect of pH on lipid accumulation by an oleaginous yeast: *Rhodotorula glutinis* IIP-30. World Journal of Microbiology and Biotechnology 8(4): 382-384.
16- Karatay S. E. and Donmez G. (2010) Improving the lipid accumulation properties of the yeast cells for biodiesel production using molasses. Bioresource Technology 101(20): 7988-7990.
17- Kraisintu P., Yongmanitchai W. and Limtong S. (2010) Selection and optimization for lipid production of a newly isolated oleaginous yeast, *Rdodosporidium toruloides* DMKU3-TK16, Kasetsart Journal (Natural Science), 44 (1): 436-445.
18- Leesing R. and Baojungharn R. (2011) Microbial Oil production by isolated oleaginous yeast *Torulaspora globosa* YU5/2. Engineering and Technology 76: 799-803.
19- Li Q., Du W. and Liu D. (2008) Perspective of microbial oils for biodiesel production. Applied Microbiology and Biotechnology 80:749-756.
20- Li Y. H., Liu B., Sun Y., Zhao Z. B. and Bai F. W. (2005) Screening of oleaginous yeasts for broad-spectrum carbohydrates assimilation capacity. China Biotechnology 25: 39-43.
21- Liang X. A., Dong W. B., Miao X. J. and Dai C. J. (2006) Production technology and influencing factors of microorganism grease. Food Research and Development 27(3): 46-47.
22- Lin-Vien D., Colthup N. B., Fateley W. G. and Grasselil J. G. (1991) The Handbook of Infrared and Raman Characteristic Frequencies of Organic Molecules. Academic Press, Inc. United Kingdom. p. 141.
23- Liu G. Q., Lin Q. L., Jin X. C., Wang X. L. and Zhao Y. (2010) Screening and fermentation optimization of microbial lipid-producing molds from forest soils. African Journal of Microbiology 4(14): 1462-1468.
24- Manuel Ageitos J., Vallejo J. A., Veiga-Crespo P. and Villa T. G. (2011) Oily yeasts as oleaginous cell factories. Applied Microbiology and Biotechnology 90(4): 1219-27.
25- Meester P. A. E. P., Huijberts G. N. M and Eggink G. (1996) High-cell-density of the lipid accumulating yeast *Cryptococcus curvatus* using glycerol as a carbon source. Applied Microbiology and Biotechnology 45: 575-579.
26- Melickova K., Roux E., Athenstaedt K., Andrea S., Daum G., Chardot T. and Nicaud J. M. (2004) Lipid accumulation, Lipid body formation and acyl coenzyme A oxidases of the yeast *Yarrowia lipolytica*. Applied and environmental microbiology 70(7): 3918-3924.
27- Meng X., Yang Xu, Zhang L., Nie Q. and Xian M. (2009) Biodiesel production from oleaginous microorganisms. Renewable Energy, 34: 1-5.
28- Mirbagheri M., Nahvi I., Emtiazi G., Mafakher L., and Darvishi F. (2012) Taxonomic Characterization and Potential Biotechnological Applications of *Yarrowia lipolytica* Isolated From Meat and Meat Products. Jundishapur Journal of Microbiology, 5(1): 346-351.
29- Mullner H. and Daum G. (2004) Dynamics of neutral lipid storage in yeast. Acta Biochimica Polonica, 51: 323-347.
30- Muniraj I. K., Xiao L., Hu Z., Zhan X. and Shi J. (2013) Microbial lipid production from potato processing wastewater using oleaginous filamentous fungi *Aspergillus oryzae*. Water Research Journal 47(10): 3477-83.
31- Pan L. X., Yang D. F., Shao L., Li W., Chen G. G. and Liang Z. Q. (2009) Isolation of oleaginous yeast from the soil and studies of their lipid-producing capacities, Food technology and Biotechnology 47: 215-220.
32- Papanikolaou S., Chevalot I., Komaitis M., Marc I. and Aggelis G. (2001) Single cell oil production by *Yarrowia lipolytica* growing on an industrial derivative of animal fat in batch *cultures*, Applied Microbiology and Biotechnology 58: 308-312.
33- Raschke D. and Knorr D. (2009) Rapid monitoring of cell size, vitality and lipid droplet development in oleaginous yeast *Waltomyces lipofer*. Journal of Microbiologocal Methods 79: 178-183.
34- Saxena R. K., Anand P., Saran S. and Isar J. (2009) Microbial production of 1,3-propanediol: recent developments and emerging opportunities, Biotechnology Advances 27: 895-913.
35- Sriwongchai S., Pokethitiyook P., Kruatrachue M., Bajwa P. K. and Lee H. (2013) Screening of selected oleaginous yeasts for lipid production from glycerol and some factors which affect lipid production by *Yarrowia lipolytica* strains, Journal of Microbiology, Biotechnology and Food Sciences 2(5): 2344-2348.
36- Syed M. A., Singh S. K., Pandey A., Kanjilal S., Prasad R. B. N. (2006) Effects of various process parameters on the production of α-

Linolenic acid in submerged fermentation, Food Technology and Biotechnology 44:282-287.
37- Tan K. H. and Gill C. O. (1985) Batch growth of *Saccharomycopsis lipolytica* on animal fats. Applied Microbiology and Biotechnology 21: 292-298.
38- Wynn P. J. and Ratledge C. (2005) Oils from microorganisms, Martek Bioscience Corporation, John Wiley and Sons Inc. 121-153pp.
39- Yan Z. and Chen J. (2003) Research advance on microbial oils and their exploitation and utilization, Journal of Cereals and Oils 7: 13-15.
40- Yi S. J. and Zheng Y. P. (2006) Research and application of oleaginous microorganism. China Foreign Energy 11(2): 90-94.
41- Zhao X., Kong X., Hua Y. (2008) Medium Optimization for lipid production through co-fermentation of Glucose and Xylose by the Oleaginous Yeast *Lipomyces Starkei*, eueropean Journal of Lipid Science and Technology 110(5): 405-412.
42- Zhu L. Y., Zong M. H. and Wu H. (2008) Efficient lipid production with *Trichosporon fermentans* and its use for biodiese19l preparation. Bioresource Technology 99: 7881-7885.

Molecular docking approach of monoamine oxidase B inhibitors for identifying new potential drugs: Insights into drug-protein interaction discovery

Salimeh Raeisi*

Department of Biology, Faculty of Science, Shahrekord University, Shahrekord, Iran

Received 16 August 2013 Accepted 14 September 2013

Abstract

Monoamine oxidase (EC, 1.4.3.4) or amine oxidoreductase catalyzes the oxidative deamination of biogenic amines. Abnormal action of the monoamine oxidase B has been associated with neurological dysfunctions including parkinson´s disorder. Monoamine oxidase B inhibitors divulged that these agents were effective in the therapeutic management of Parkinson's disease. Understanding the interaction of monoamine oxidase binding site with inhibitors is crucial for the development of pharmaceutical agents. At the molecular docking, the exact prediction of the binding modes between the inhibitors and protein is of central importance in structure-based drug design. In the current study, we examined two classes of monoamine oxidase B inhibitors. We applied Autodock tools 4.2, in order to set up the docking runs and predict the inhibitors binding free energy. The final product of molecular docking was clustered to specify the binding free energy and optimal docking energy conformation that is investigated as the best docked structure. Docking results indicate that the contribution of van der Waals interactions is greater than electrostatic interactions so that, it can be concluded that all of the inhibitors attached to a hydrophobic binding site in monoamine oxidase B. Among the total of molecules tested, it was proved that 2-(2-cycloheptylidenehydrazinyl)-4-(2,4-dichlorophenyl)-1,3-thiazole has the lowest binding free energy and the lowest Van der Waals energy and also the lowest inhibition constant and subsequently the most experimental affinity. As well as, we find out a possible relationship between the estimated results and experimental data. The selective information from this work is crucial for the rational drug design of more potent and selective monoamine oxidase B inhibitors based on the 8-benzyloxycaffeine scaffold.

***Keywords*:** monoamine oxidase B inhibitor, Parkinson´s disorder, molecular docking, binding free energy

Introduction

Monoamine oxidase (EC, 1.4.3.4) or amine oxidoreductase is a mitochondrial bound enzyme that contains flavinadenosine dinucleotide; monoamine oxidase catalyzes the oxidative deamination of biogenic amines, including exogenous amines, dietary amines, hormones, dopamine, serotonin and neurotransmitters (Coelho Cerqueira et al., 2010; Herraiz and Chaparro, 2005). Therefore, monoamine oxidases are virtually associated with higher brain functions. Two isoforms of monoamine oxidases have been described, i.e. monoamine oxidase A and monoamine oxidase B. Before their molecular characterization, the differences between these two isoforms were determined on the basis of substrate and inhibitor sensitiveness. Monoamine oxidase A selectively catalyzes the oxidation of norephinephrine and serotonin and is inhibited by clorgyline, whereas monoamine oxidase B selectively catalyzes the oxidation of benzylamine and phenylethylamine and is inhibited by deprenyl (Lewis et al., 2007; Nagatsu, 2004; Oreland, 2004). Abnormal action of the monoamine oxidase B isoform has been associated with neurological dysfunctions including parkinson´s disorder and alzheimer´s disorder whereas the monoamine oxidase A isoform seems to be associated with psychiatric considerations including depression and cardiac cellular degeneration (Bortolato et al., 2008). Furthermore, reports have described that the level of monoamine oxidase B in human beings raises four to five fold throughout aging and results in an increase in catalytic reaction products such as hydrogenperoxide and a decrease in certain neurotransmitter levels (Bortolato et al., 2008; Herraiz and Chaparro, 2005). Monoamine oxidase B inhibitors, such as D-deprenyl (selegiline) divulged that these agents were effective in the therapeutic management of Parkinson's disease. The rationale utilization of monoamine oxidase B inhibitors in parkinson's disorder is based on the concept that dopamine is deaminated by monoamine oxidase B. Inhibition of monoamine oxidase B about an increases the dopamine, and low levels of dopamine is associated with

∗Corresponding author E-mail:
salimeh.raeisi@stu.sku.ac.ir

parkinson´s disease. Age related additions in monoamine oxidase B function, also the neuroprotective impressions of its inhibitors, have been studied as rational bases to apply monoamine oxidase B inhibitors in alzheimer's disorder (Bortolato et al., 2008; Jensen et al., 2006; Luhr et al., 2010). Regrettably, the usage of monoamine oxidase inhibitors might be confined, although they are often last line treatment, in some cases, by adverse effects such as those related to the co-administration of certain diets or drugs, which can lead to serious hypertensive and hyperpyretic crises (Bortolato et al., 2008). Hence, tremendous attempts have been undertaken to discover new pharmaceutical agent that are linked to monoamine oxidase inhibition. Hence, recognition of monoamine oxidase B inhibitors is a great interest in drug discovery (Geldenhuys et al., 2012).

Materials and Methods

Understanding the interactions of monoamine oxidase binding site with inhibitors are crucial for the development of pharmaceutical agents. Computer aided drug design is an applicable method that can study these interactions and describe significant characteristics for monoamine oxidase binding site recognition (Delogu et al., 2011; Harkcom and Bevan, 2007). Automated docking is widely applied for approximation of bio molecular complex and in order to analyze the structure-function processes and the bio molecular design. Drug design is the other application of docking. The precise interaction of agents or candidate molecules with their targets is crucial in the developmental procedure. Docking is applied to predict the binding orientation of small molecular drug candidates to protein targets, subsequently predicting the affinity and activity of the drug candidates (Goodsell, 2009; Morris et al., 2009; Morris et al., 2008). In addition, docking is often applied to predict binding affinities of drug candidates in virtual screening experiments and in considering structure-activity relationships to prioritize synthesis of new drugs (Wu et al., 2003). Docking of the small molecules into the structures of macromolecular targets and scoring their potential complementarity to binding site is widely applied in hit recognition new drugs. Indeed, there are a number of drugs whose development was heavily based on or influenced by structure-based drug design and screening strategies.

In the present work, our purpose was to distinguish correct poses of inhibitor in the binding pocket of monoamine oxidase B and to predict the affinity between the inhibitor and monoamine oxidase B. In other words, in this study docking procedure describes a process by which two molecules fit together in three-dimensional space (Kitchen et al., 2004). At the molecular docking, the exact prediction of the binding modes between the inhibitors and protein is of central importance in structure-based drug design (Taylor et al., 2002).

Ligand structure

Due to the special characteristics of monoamine oxidase, the researchers have focused on various aspects of it (Carroll et al., 2011; Chimenti et al., 2005; Chimenti et al., 2009; Chimenti et al., 2006; Delogu et al., 2011; Mu et al., 2012; Reniers et al., 2011; Strydom et al., 2010; Van der Walt et al., 2009). Since, some of these were the effective inhibitors against the monoamine oxidase B it may be a potential therapeutic agent for parkinson´s disease. Therefore, we select some of the potent inhibitors for the docking studies against monoamine oxidase B (Scheer et al., 2011; Strydom et al., 2010). In the current study, we examine two classes of monoamine oxidase B inhibitors; these two classes of inhibitors are 2-(2-cycloheptylidene hydrazinyl) and methyl cyclohexylidene hydrazinyl derivatives (8-benzyloxycaffeine analogues). Figure 1 shows the structure of inhibitors A1-A6 and figure 2 shows the structure of inhibitors B1-B5.

In the present study, molecular modeling of the inhibitors was carried out using Hyperchem 7 software. Hyperchem 7 was employed to draw and optimize the structure of inhibitors (Ivanciuc, 1996) For all initial structures geometric optimization calculations by use of molecular mechanics were performed and afterward the lowest energy conformers were optimized using the semiempirical PM3 method, the conjugate gradient and steepest descent algorithm. At the end these structures converted to .pdb format by Hyperchem 7 software. Optimized inhibitor structure was used as input file for docking (Froimowitz, 1993).

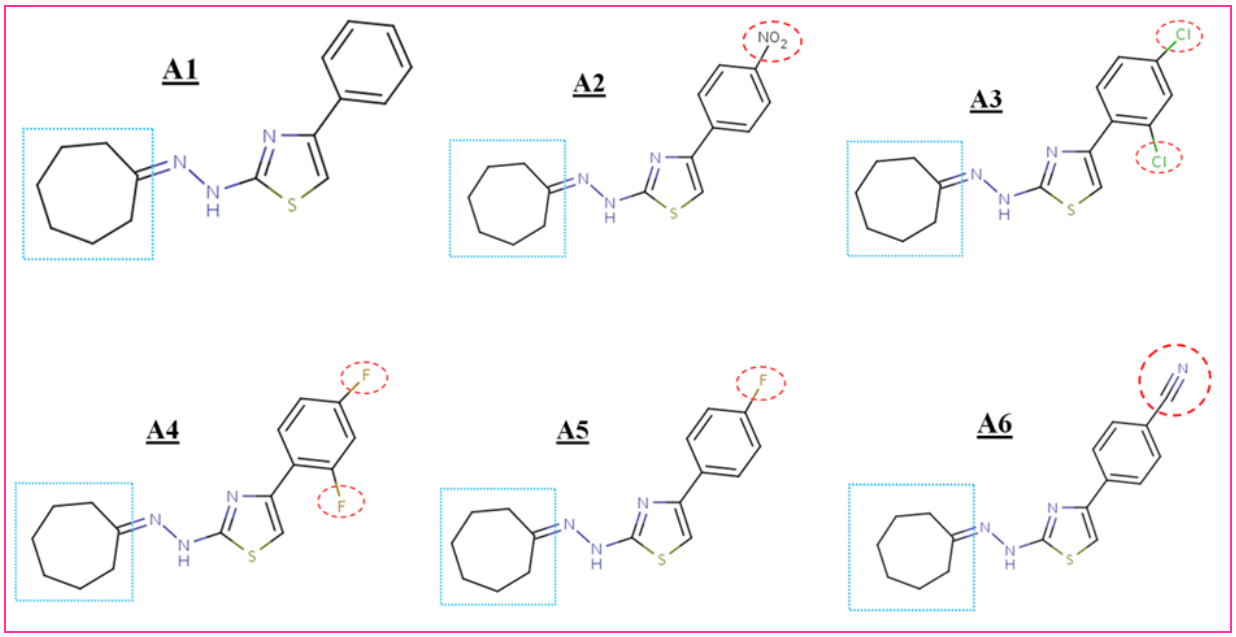

Figure 1. Structure of inhibitors A1-A6. [A1] 2-(2-cycloheptylidenehydrazinyl)-4-phenyl-1,3-thiazole, [A2] 2-(2-cycloheptylidenehydrazinyl)-4-(4-nitrophenyl)-1,3-thiazole, [A3] 2-(2-cycloheptylidenehydrazinyl)-4-(2,4-dichlorophenyl)-1,3-thiazole, [A4] 2-(2-cycloheptylidenehydrazinyl)-4-(2,4-difluorophenyl)-1,3-thiazole, [A5] 2-(2-cycloheptylidenehydrazinyl)-4-(4-fluorophenyl)-1,3-thiazole, [A6] 4-[2-(2-cycloheptylidenehydrazinyl)-1,3-thiazol-4-yl]benzonitrile.

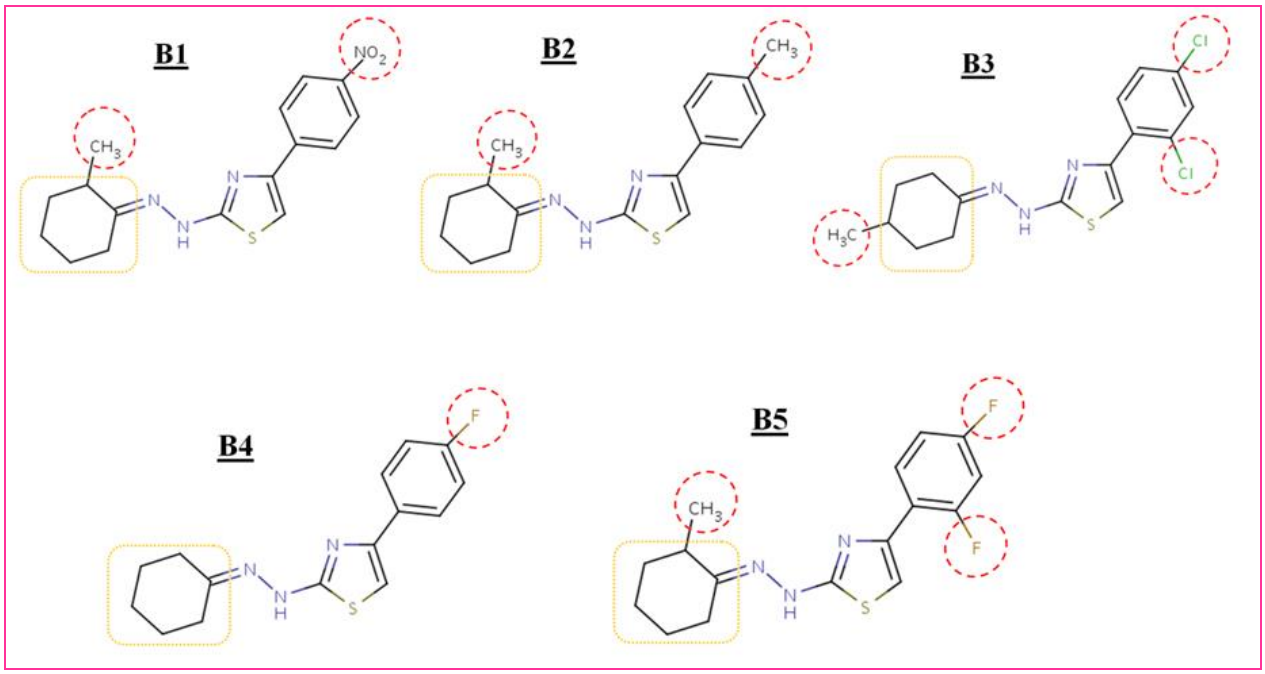

Figure 2. Structure of inhibitors B1-B5. [B1] 2-[(2E)-2-(2-methylcyclohexylidene)hydrazinyl]-4-(4-nitrophenyl)-1,3-thiazole, [B2] 2-[(2E)-2-(2-methylcyclohexylidene)hydrazinyl]-4-(4-methylphenyl)-1,3-thiazole, [B3] 4-(2,4-dichlorophenyl)-2-[2-(4-methylcyclohexylidene)hydrazinyl]-1,3-thiazole, [B4] 2-(2-cyclohexylidenehydrazinyl)-4-(4-fluorophenyl)-1,3-thiazole, [B5] 4-(2,4-difluorophenyl)-2-[(2E)-2-(2-methylcyclohexylidene)hydrazinyl]-1,3-thiazole.

Protein structure

In the current study, the protein X-ray crystal structure of human monoamine oxidase B with 1OJA code and X-ray diffraction at 1.70 Å resolution was received from the Protein Data Bank and was used as the receptor starting structure. This structure comprised a dimeric form of the human monoamine oxidase B, with each chain interacting

with FAD and a co-crystallized inhibitor codenamed ISN (isatin or indol-2,3-dione) and several water molecules. Figure 3 shows the x-ray crystal structure of monoamine oxidase B in complex with inhibitor ISN and FAD. For docking process, only the coordinates of chain A and FAD were considered as the receptor structure, and the co-crystallized inhibitor was removed for the docking studies. The presence of cofactors revealed to be essential for the definition of the docking site. We applied Autodock tools 4.2, in order to set up the docking runs and predict the inhibitors binding free energy.

Docking protocol

In the current study, AutoDockTools 4.2 was applied for docking process. AutoDockTools 4.2 uses a grid-based approach in order to allow exploring of the large conformational space available to drug candidate around an embedded protein in a grid, as well as to provide rapid evaluation of the binding energy of drug candidate conformations. A probe atom is consecutively located at each grid point, the interaction energy between the probe and the target protein is estimated, and the value is stored in the grid. This grid of energies may then be applied as a lookup table during the docking simulation (Morris et al., 2009; Morris et al., 2008)**.**

AutoDockTools 4.2 was employed to docking process of inhibitors to monoamine oxidase B (Morris et al., 2009). Initially, all of the polar hydrogens were added to the inhibitors and Gasteiger-Marsili atomic partial charges were set for them, and all the inhibitors rotatable bonds were adjusted in fewest atoms. The final inhibitor structures were saved in .pdbqt format. Then polar hydrogen was added to the protein crystal structure and the kollman atomic partial charge was set for monoamine oxidase B. The final protein structure was saved in .pdbqt format. An extended pdb format, called pdbqt, is applied for coordinate files, which include atomic partial charges and atom types; pdbqt files as well include data on the torsional degrees of freedom (Morris et al., 2008). Grid box was created by Autogrid 4 with 30 × 30 × 30 Å in x, y and z directions with 0.375 Å spacing and center of box was located on the active site according to co-crystallized inhibitor coordination. The monoamine oxidase B active site was easily distinguished as the hydrophobic cavity comprising the co-crystallized ligand ISN. The genetic algorithm was used to determine the probable accommodate for each inhibitor to monoamine oxidase B. Docking was performed with Lamarckian genetic algorithm (Genetic Algorithm combined with a local search) with population size of 150. Monoamine oxidase B kept rigid in docking process. The inhibitor structures were attributed flexible. In other words all the inhibitors rotatable bonds were adjusted in fewest atoms; note also that cyclic rotatable bonds are excluded. The other parameters were used as default docking parameters, except for the step size parameters that were chosen to be 0.2 (translation) and 5.0 degrees (quaternion and torsion). Finally, by setting all the parameters, inhibitors were docked to the monoamine oxidase B (Chimenti et al., 2004; Coelho Cerqueira et al., 2010; Harkcom and Bevan, 2007).

AutoDockTools contain a number of methods for considering the results of docking simulations, including tools for clustering results by conformational resemblance, visualizing conformations, visualizing interactions between ligands and proteins. At the end of a docking process, AutoDock writes the data on clustering and binding energies to the log file. The docking results were clustered with 2 Å root mean square deviation and were ranked according to the estimated binding free energy. The structure with proportional lower binding free energy and the most conformation in cluster was selected for the optimum docking conformation (Goodsell, 2009).

The intensity of the interaction between the inhibitor and the receptor can be evaluated experimentally and is often described as the dissociation constant, Kd, or by the concentration of inhibitor that inhibits activity by 50%, the IC50. The binding free energy is the thermodynamic quantity that is determined by equation 1 and is of interest in computational structure-based design (Brooijmans, 2009).

Equation 1

$$\Delta G_{bind} = \Delta G_{complex} - \left(\Delta G_{ligand} - \Delta G_{receptor}\right)$$

The relationship between the binding free energy ΔG and the experimentally determined Kd or IC50 is demonstrated in equation 2.

Equation 2

$$\Delta G_{bind} = -RT \ln K_{eq} = -RT \ln K_d = -RT \ln 1/IC_{50}$$

The interactions between the inhibitor and the receptor also can be measured by means of AutoDock 4.2. In the present work, our purpose was to attain an agreement between the docking results and experimental data.

The AutoDock 4.2 force field is designed to estimate the binding free energy of inhibitors to protein. It includes an updated charge-based

desolvation term, advances in the directionality of hydrogen bonds, and various improved models of the unbound state. AutoDock 4.2 applies a semi-empirical free energy force field and grid-based docking to assess conformations during docking process. Equation 3 represent the docking binding free energy, this formula automatically was computed by AutoDock 4.2 (Morris et al., 2008).

Equation 3

$$\Delta G_{binding} = [\Delta G_{intermolecular} + \Delta G_{internal} + \Delta G_{tors}] - [\Delta G_{unbound}]$$

In the above formula, the final intermolecular energy is calculated with equation 4, so that the final intermolecular energy involves in van der Waals, hydrogen bonding, desolvation and electrostatic contribution between the inhibitor and the protein binding site.

Equation 4

$$\Delta G_{intermolecular} = [\Delta G_{vdw} + \Delta G_{hbond} + \Delta G_{desolv}] + \Delta G_{elec}$$

Results

Molecular docking was applied to describe and find out the binding sites in monoamine oxidase B. The final product of molecular docking, as the best docked structure was clustered to specify the binding free energy and optimal docking energy conformation. As well as we consider the molecular docking results to elucidate their binding mode in the monoamine oxidase B.

Table 1 summarizes the docking results. In this study the inhibition constant (Ki) and the RMSD value for drug-like molecules were also determined. Negative values of predicted free energies of binding show that all inhibitors correctly docked to the crystal structure of the monoamine oxidase B. Docking results also indicate that the contribution of van der Waals interactions is greater than electrostatic interactions so that, it can be concluded that all of the inhibitors attached to a hydrophobic binding site in monoamine oxidase B. In other words, the non-polar interactions between monoamine oxidase B and inhibitors are the main factor in the connectivity features and they are the dominant component contributing to the binding affinity. Among the molecules tested of A class, A3 or 2-(2-cycloheptylidenehydrazinyl)-4-(2,4-dichlorophenyl)-1,3-thiazole demonstrated the lowest binding free energy (-11.96 kcal/mol). As well as, among the molecules tested of B class, B3 or 4-(2,4-dichlorophenyl)-2-[2-(4-methylcyclohexylidene)hydrazinyl]-1,3-thiazole demonstrated the lowest binding free energy (-11.54 kcal/mol). The more negative is the free binding energy, the more potent is the interaction.

According to the table 1, among the total of molecules tested, it was proved that A3 has the lowest binding free energy (-11.96 kcal/mol), Van der Waals energy (-13.14 kcal/mol) and also the lowest inhibition constant (1.70 n M) and subsequently the most experimental affinity. It was proved that after A3, B3 also has the lowest binding free energy (-11.54 kcal/mol), the lowest Van der Waals energy (-12.69 kcal/mol), the lowest inhibition constant (3.50 n M) and the most experimental affinity. In other words, A3 and B3 have the highest interactions and the more potential binding affinity for the enzyme binding site.

Special attention has been devoted to the substituent at thiazole ring. 2,4-dichlorophenyl substitution leads to the highest potential binding affinity at 2-(2-cycloheptylidenehydrazinyl) and methyl cyclohexylidene hydrazinyl derivatives. It has been found clearly that, in the presence of a dichlorophenyl substituent in the 2,4 position, the potency of inhibitor was increased.

The active site is frequently known from crystal structures of ligand-bound receptors. The distinguishing of active sites can play a central role in realizing protein function (Brooijmans, 2009).

The docking results indicate that all inhibitors bind to monoamine oxidase B active site; active site is a hydrophobic pocket that was surrounded by the aromatic and aliphatic residues. The active site of monoamine oxidase B constitutes of an entrance cavity and substrate cavity; depending on the nature of the ligand, two cavities can be separated or joined (Chimenti et al., 2004; Harkcom and Bevan, 2007).

In structure-based design, the known or predicted shape of the binding site is used to optimize the inhibitor as a best fit to the receptor. As well as, the orientations of these inhibitors in the active site are very important, with their Ki values, for rational drug design. In most of the cases, careful observations of the figures divulge that inhibitor positioning in the active site sits reasonably well. The binding manners and geometrical orientation of all compounds in the binding site were nearly identical, hence proposing that all the inhibitors have the same interactions with enzyme and occupied a common space in the receptor. Hydrophobic cavity of binding site constitutes the inner cavity of the active site, and comprises the residues such as Tyr 60, Leu171, Ile198, Gln206, Tyr326, Leu328, Phe343, Tyr398, Tyr435. Fig 4 shows the lowest energy configuration of A3-monoamine oxidase B complex. Observations of the docked conformation of A3 demonstrated

interactions with many residues; in this complex, A3 was located inside the cavity that comprising the residues such as Gly57, Gly58, Leu171, Ile198, Gln206, Tyr326, Phe343, Tyr398, Thr426, Gly434, Tyr435, Met436. And Fig 5 shows the lowest energy configuration of B3-monoamine oxidase B complex, B3 was located inside the cavity that containing the residues such as Gly57, Gly58, Tyr60, Leu171, Gln206, Tyr326, Phe343, Tyr398, Thr426, Gly434, Tyr435, Met436.

Other interactions proposed by the docking consequences were the hydrophobic interactions of the inhibitors hydrophobic groups, as they were observed oriented towards the co-crystallized ligand ISN, so that they have similar hydrophobic interactions. Fig 6-A shows the best virtual docking pose of A3 and the superimposition of A3 and ISN, and Fig 6-B shows the best virtual docking pose of B3 and the superimposition of B3 and ISN. In this docked conformation, the A3 and B3 interact with flavin moiety of the FAD via a hydrogen bond and show tight interactions with Gln206, Tyr326, Phe343, Tyr398 and Tyr435 (Fig 6 A-B). For superimposition of A3 and B3 with ISN, the indol ring is located between Tyr435 and Tyr398 in the hydrophobic cavity with an upright conformation to flavin ring of FAD. Therefore, AutoDock 4.0 viewed as reliable for docking A3 and B3, and related compounds into monoamine oxidase B.

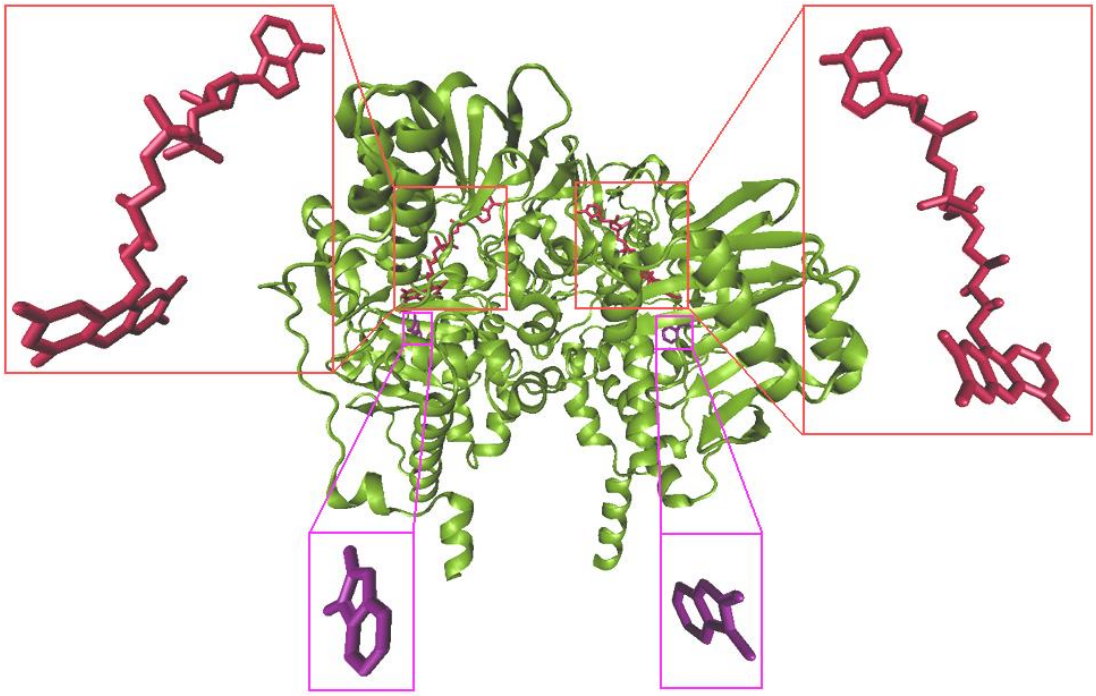

Figure 3. X-ray crystal structure of monoamine oxidase B in complex with inhibitor ISN (purple) and FAD (red).

Table 1. Autodock's binding free energy derived from the docking studies on monoamine oxidase B.

Inhibitor Index	$\Delta G_{binding}$	Ki	ΔG_{vdW}	ΔG_{ele}	ΔG_{inter}	ΔG_{tors}	$\Delta G_{unbound}$	RMSD	IC50
A1	-11.63	3.01	-12.82	-0.00	+0.05	+1.19	+0.05	160.981	2.7e-05
A2	-11.05	7.90	-12.13	-0.41	-0.16	+1.49	-0.16	159.024	1.1e-05
A3	-11.96	1.70	-13.14	-0.01	+0.12	+1.19	+0.12	159.562	0.00094
A4	-10.72	32.51	-11.43	+0.02	+0.04	+1.19	+0.04	156.675	1.6e-05
A5	-9.73	74.19	-10.67	+0.05	+0.57	+0.89	+0.57	155.853	4e-06
A6	-11.32	5.07	-12.50	-0.01	+0.01	+1.19	+0.01	159.498	4.6e-05
B1	-11.23	5.84	-12.34	-0.39	+0.00	+1.49	+0.00	157.532	3.2e-05
B2	-10.21	32.87	-11.39	-0.01	+0.17	+1.19	+0.17	157.254	0.000143
B3	-11.54	3.50	-12.69	-0.04	+0.14	+1.19	+0.14	160.077	0.009446
B4	-9.91	54.84	-11.13	+0.03	-0.16	+1.19	-0.16	156.619	4e-06
B5	-9.98	48.38	-11.17	-0.00	+0.12	+1.19	+0.12	156.271	1.4e-05

Abbreviations: ΔGbinding, Estimated Free Energy of Binding (kcal/mol); ΔGvdw, vander Waals or Lennard–Jones potential factor of binding free energy (kcal/mol); ΔGelec, electrostatic factor of binding free energy (kcal/mol); ΔGinter, Gibbs free energy of binding (kcal/mol); ΔGtors, torsional energy of binding (kcal/mol); ΔGunbound, unbound System's energy (kcal/mol); Ki, inhibition constant (nM); RMSD, reference root mean square deviation ; IC50 refers to the experimental predicted activity (mM). Refrence of inhibitor (Scheer et al., 2011; Strydom et al., 2010).

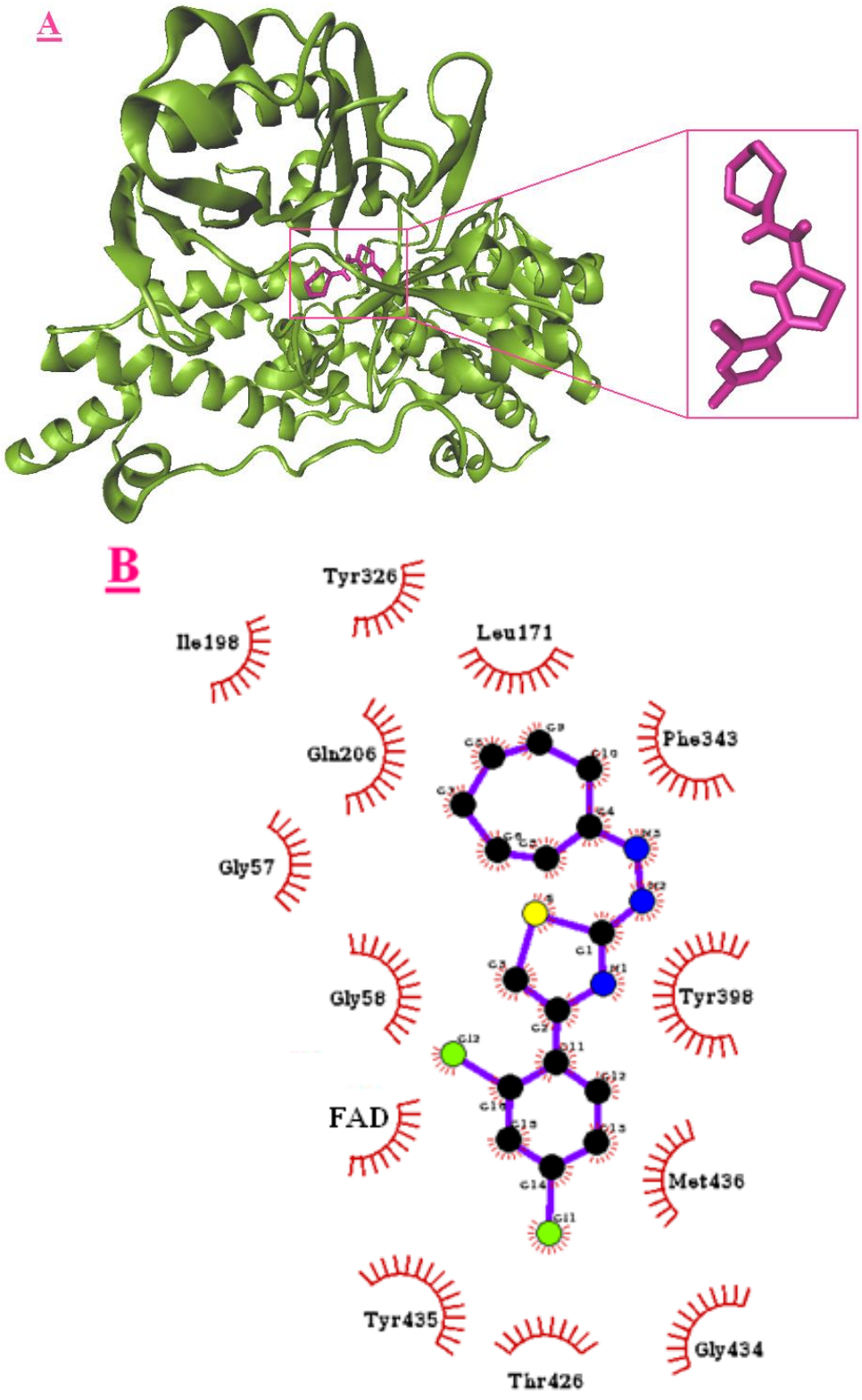

Figure 4. Docking result of A3 (magenta) with monoamine oxidase B. The lowest energy configuration of A3-monoamine oxidase B complex is demonstrated in VMD(A) and Ligplot (B) presentations. In Ligplot presentations (B), carbons are in black, nitrogens in blue and oxygens in red.

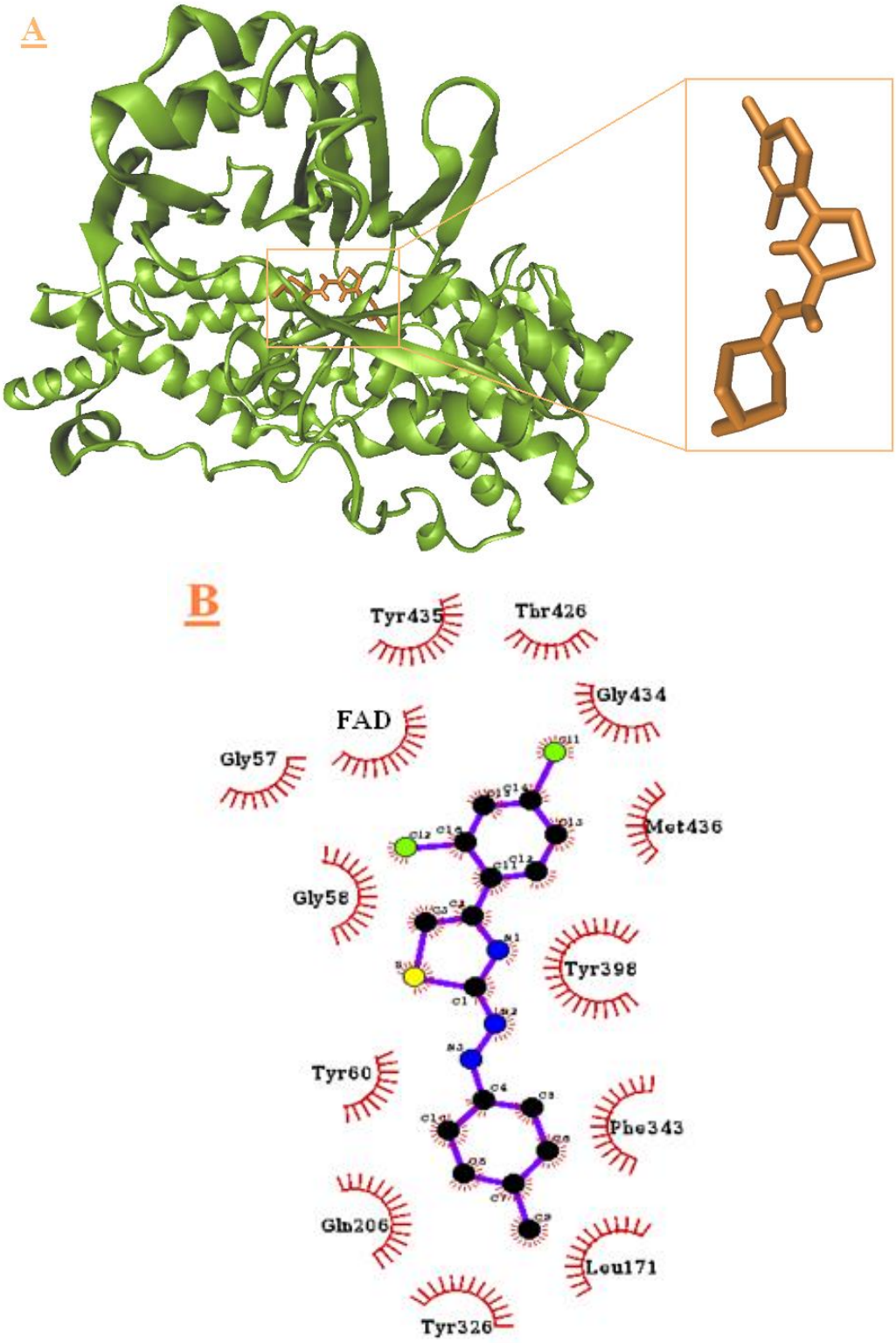

Figure 5. Docking result of B3 (orange) with monoamine oxidase B. The lowest energy configuration of B3-monoamine oxidase B complex is demonstrated in VMD(A) and Ligplot (B) presentations. In Ligplot presentations (B), carbons are in black, nitrogens in blue and oxygens in red.

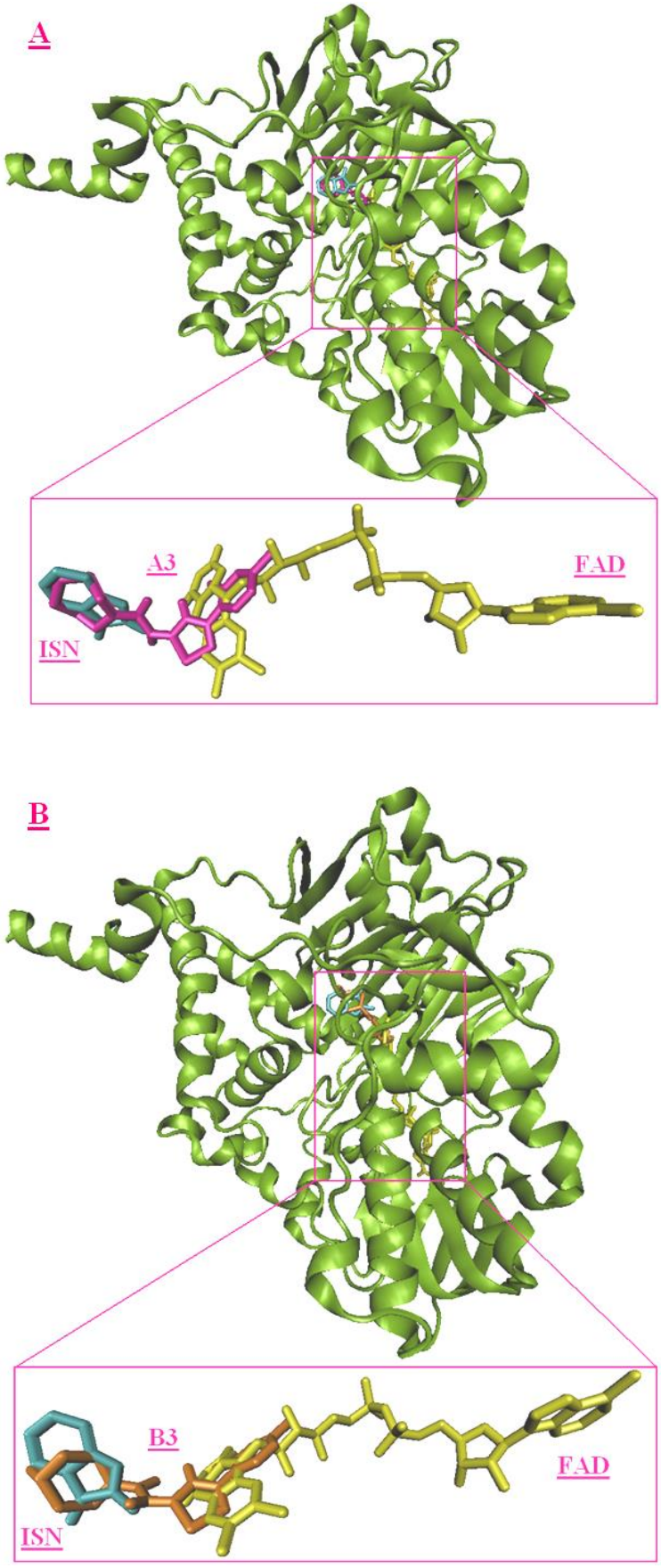

Figure 6. Best virtual docking pose of A3 and B3. (A), superimposition of A3 (magenta) and FAD (red) and ISN (purple); (B) superimposition of B3 (orange) and FAD (red) and ISN (purple).

Discussion

The target of this study was to carry out molecular docking to estimate the binding free energies and inhibition constants of tested monoamine oxidase B inhibitors and to compare these computational results with those of the experimentally obtained results.

In the resent study, we employed computational approaches, such as molecular docking to estimate the binding free energy of two classes of monoamine oxidase B inhibitors. Compare with the van der Waals and electrostatic energies for these components showed a significant share of the van der Waals energies. Our results clearly showed that non polar interactions play a significant role in determining the binding free energy. Our findings propose that (2,4-dichlorophenyl)-1,3-thiazole might demonstrate a crucial scaffold for the development of monoamine oxidase inhibitors. All inhibitors bind to monoamine oxidase B active site and subsequently inhibit it. So that they have potent affinity to the monoamine oxidase B and thus they can behave like as the pharmaceutical agents. Among the tested derivatives we preferred A3 and B3 as potent anti monoamine oxidase B agents. Understanding, an atomic-level of the catalytic and inhibition mechanisms of monoamine oxidase B could assist to search for rationally-designed inhibitors of monoamine oxidase B, and would be of significant importance monoamine oxidase B activity. In the present work, our purpose was to attain an agreement between the docking results and experimental data. We discovered good relationship between the estimated results and experimental data. The selective information from this work is crucial for the rational drug design of more potent and selective monoamine oxidase B inhibitors based on the 8-benzyloxycaffeine scaffold. Such observations can also help to study 8-benzyloxycaffeine, by increased metabolism of biogenic amines within some key areas of the central nervous system, as an effective scaffold for rational design of novel and potential drugs against diseases precipitated.

Note: All the figures are color in online version.

Acknowledgment

I thank to the Golestan University for their financial support to perform this work.

References

1- Bortolato M., Chen K. and Shih J. C. (2008) Monoamine oxidase inactivation: from pathophysiology to therapeutics. Advanced drug delivery reviews 60:1527-1533.

2- Brooijmans N. 2009. Docking methods, ligand design and validating data sets in the structural genomics era. *In* Structural Bioinformatics. J.G.a.P.E. Bourne, editor. John Wiley & Sons.

3- Carroll R. T., Dluzen D. E., Stinnett H., Awale P. S., Funk M. O. and Geldenhuys W. J. (2011) Structure-activity relationship and docking studies of thiazolidinedione-type compounds with monoamine oxidase B. Bioorganic & medicinal chemistry letters 21:4798-4803.

4- Chimenti F., Maccioni E., Secci D., Bolasco A., Chimenti P., Granese A., Befani O., Turini P., Alcaro S. and Ortuso F. (2005) Synthesis, molecular modeling studies, and selective inhibitory activity against monoamine oxidase of 1-thiocarbamoyl-3, 5-diaryl-4, 5-dihydro-(1 H)-pyrazole derivatives. Journal of medicinal chemistry 48:7113-7122.

5- Chimenti F., Secci D., Bolasco A., Chimenti P., Bizzarri B., Granese A., Carradori S., Yanez M., Orallo F. and Ortuso F. (2009) Synthesis, Molecular Modeling, and Selective Inhibitory Activity against Human Monoamine Oxidases of 3-Carboxamido-7-Substituted Coumarinsâ€ Journal of medicinal chemistry 52:1935-1942.

6- Chimenti F., Secci D., Bolasco A., Chimenti P., Granese A., Befani O., Turini P., Alcaro S. and Ortuso F. (2004) Inhibition of monoamine oxidases by coumarin-3-acyl derivatives: biological activity and computational study. Bioorganic & medicinal chemistry letters 14:3697-3703.

7- Chimenti F., Secci D., Bolasco A., Chimenti P., Granese A., Carradori S., Befani O., Turini P., Alcaro S. and Ortuso F. (2006) Synthesis, molecular modeling studies, and selective inhibitory activity against monoamine oxidase of N-bis [2-oxo-2-H-benzopyran]-3-carboxamides. Bioorganic & medicinal chemistry letters 16:4135-4140.

8- Coelho Cerqueira E., Netz P. A., Diniz C., Petry do Canto V. and Follmer C. (2010) Molecular insights into human monoamine oxidase (MAO) inhibition by 1, 4-naphthoquinone: Evidences for menadione (vitamin K3) acting as a competitive and reversible inhibitor of MAO. Bioorganic & medicinal chemistry 19:7416-7424.

9- Delogu G., Picciau C., Ferino G., Quezada E., Podda G., Uriarte E. and Vina D. (2011) Synthesis, human monoamine oxidase inhibitory activity and molecular docking studies of 3-heteroarylcoumarin derivatives. European journal of medicinal chemistry 46:1147-1152.

10- Froimowitz M. (1993) HyperChem: a software package for computational chemistry and molecular modeling. BioTechniques 14:1010-1013.

11- Geldenhuys W. J., Funk M. O., Van der Schyf C. J. and Carroll R. T. (2012) A scaffold hopping approach to identify novel monoamine oxidase B inhibitors. Bioorganic & medicinal chemistry letters 22:1380-1383.

12- Goodsell D. S. (2009) Computational docking of biomolecular complexes with AutoDock. Cold Spring Harbor protocols 2009:pdb prot5200.
13- Harkcom W. T. and Bevan D. R. (2007) Molecular docking of inhibitors into monoamine oxidase B. Biochemical and biophysical research communications 360:401-406.
14- Herraiz T. and Chaparro C. (2005) Human monoamine oxidase is inhibited by tobacco smoke: b-carboline alkaloids act as potent and reversible inhibitors. Biochemical and Biophysical Research Communications 326:378–386.
15- Ivanciuc O. (1996) HyperChem Release 7 for Windows. Journal of chemical information and computer sciences 36:612-614.
16- Jensen S. B., Olsen A. K., Pedersen K. and Cumming P. (2006) Effect of monoamine oxidase inhibition on amphetamine evoked changes in dopamine receptor availability in the living pig: A dual tracer PET study with [11C] harmine and [11C] raclopride. Synapse 59:427-434.
17- Kitchen D. B., Decornez H. l. n., Furr J. R. and Bajorath J. r. (2004) Docking and scoring in virtual screening for drug discovery: methods and applications. Nature reviews Drug discovery 3:935-949.
18- Lewis A., Miller J. H. and Lea R. A. (2007) Monoamine oxidase and tobacco dependence. Neurotoxicology 28:182-195.
19- Luhr S., Vilches-Herrera M., Fierro A., Ramsay R. R., Edmondson D. E., Reyes-Parada M., Cassels B. K. and Iturriaga-Vasquez P. (2010) 2-Arylthiomorpholine derivatives as potent and selective monoamine oxidase B inhibitors. Bioorganic & medicinal chemistry 18:1388-1395.
20- Morris G. M., Huey R., Lindstrom W., Sanner M. F., Belew R. K., Goodsell D. S. and Olson A. J. (2009) AutoDock4 and AutoDockTools4: Automated docking with selective receptor flexibility. Journal of computational chemistry 30:2785-2791.
21- Morris G. M., Huey R. and Olson A. J. (2008) Using AutoDock for ligand-receptor docking. Current protocols in bioinformatics / editoral board, Andreas D. Baxevanis ... [et al.] Chapter 8:Unit 8 14.
22- Mu L.-H., Wang B., Ren H.-Y., Liu P., Guo D.-H., Wang F.-M., Bai L. and Guo Y.-S. (2012) Synthesis and inhibitory effect of piperine derivates on monoamine oxidase. Bioorganic & medicinal chemistry letters.
23- Nagatsu T. (2004) Progress in monoamine oxidase (MAO) research in relation to genetic engineering. Neurotoxicology 25:11-20.
24- Oreland L. (2004) Platelet monoamine oxidase, personality and alcoholism: the rise, fall and resurrection. Neurotoxicology 25:79-89.
25- Reniers J., Meinguet C., Moineaux L., Masereel B., Vincent S. P., Frederick R. and Wouters J. (2011) Synthesis and inhibition study of monoamine oxidase, indoleamine 2, 3-dioxygenase and tryptophan 2, 3-dioxygenase by 3, 8-substituted 5 H-indeno [1, 2 c] pyridazin-5-one derivatives. European journal of medicinal chemistry 46:6104-6111.
26- Scheer M., Grote A., Chang A., Schomburg I., Munaretto C., Rother M., Sohngen C., Stelzer M., Thiele J. and Schomburg D. (2011) BRENDA, the enzyme information system in 2011. Nucleic acids research 39:D670-676.
27- Strydom B., Malan S. F., Castagnoli N., Bergh J. J. and Petzer J. P. (2010) Inhibition of monoamine oxidase by 8-benzyloxycaffeine analogues. Bioorganic & medicinal chemistry 18:1018-1028.
28- Taylor R. D., Jewsbury P. J. and Essex J. W. (2002) A review of protein-small molecule docking methods. Journal of Computer-Aided Molecular Design 16:151–166.
29- Van der Walt E. M., Milczek E. M., Malan S. F., Edmondson D. E., Castagnoli Jr N., Bergh J. J. and Petzer J. P. (2009) Inhibition of monoamine oxidase by (E)-styrylisatin analogues. Bioorganic & medicinal chemistry letters 19:2509-2513.
30- Wu G., Robertson D. H., Brooks C. L. and Vieth M. (2003) Detailed analysis of gridbased molecular docking: A case study of C-DOCKER. A CHARM based MD docking algorithm. Journal of computational chemistry 24:1549-1562.

A survey on optimization of *Agrobacterium*-mediated genetic transformation of the fungus *Colletotrichum gloeosporioides*

Mahsa Yousefi-Pour Haghighi[1], Jalal Soltani[2]*, Sonbol Nazeri[1]

1. Plant Biotechnology Department, Bu-Ali Sina University, Hamedan, Iran
2. Phytopathology Department, Bu-Ali Sina University, Hamedan, Iran

Received 15 July 2013 Accepted 01 September 2013

Abstract

The fungus *Colletotrichum gloeosporioides* is the causative agent of anthracnose disease of many tropical, subtropical and temperate fruits, and a microbial source of the anticancer drug, Taxol. Here, we introduce an optimized *Agrobacterium tumefaciens*-mediated transformation (ATMT) protocol for genetic manipulation of this fungus using *hph* and *gfp*-tagged *hph* genes as selection markers. Results showed that falcate spores can be easily used instead of protoplasts for transformation. Several experimental parameters were shown to affect transformation efficiencies, among which the length of co-cultivation, the ratio of fungal conidia to bacterium during co-cultivation, the kind of membrane during co-cultivation, and the kind of fungal growth medium during transformants selection, showed the highest influences on ATMT frequencies. Results indicated that the optimal ATMT of *C. gloeosporioides* was achived after 3 days of co-cultivation, at 10^7 per ml fungal conidia, via the use of Fabriano 808 filter paper and Czapek's culture medium. Successive subculturing of transformants on selective and non-selective media demonstrated the stable expression of transgens, and subsequent PCR based analyses of transformants revealed the presence (100%) of transferred genes. Flourescence microscopy analyses showed a punctuate pattern for localization of an expressed Gfp-tagged Hph protein inside fungal hyphae. The optimized ATMT protocol generated mutants that showed different phenotypes based on their vegetation and pigmentation. This suggests the possible applicability of this technique for functional genetics studies in *C. gloeosporioides*, through insertional mutagenesis.

Keywords**:** *Colletotrichum gloeosporioides; Agrobacterium tumefaciens;* ATMT*;* Genetic transformation*;* Insertional mutagenesis

Introduction

Colletotrichum is one of the most common and important genera of filamentous fungi, that cause post-harvest rots, anthracnose spots, and blights of aerial plant parts. Members of this genus cause major economic losses, especially in fruits, vegetables, and ornamentals (Damm et al., 2010). The plant pathogenic fungus *Colletotrichum gloeosporioides* (Penz) Penz & Sacc in Penz,, is the causal agent of anthracnose on many tropical, subtropical and temperate fruits (Waller, 1992; Freeman and Shabi, 1996), especially in *Citrus* species, including oranges, tangerines, navel oranges, and grapefruits. Post-harvest problems caused by *C. gloeosporioides* are particularly prevalent in the tropics, where they are often a significant factor in limiting export (Fitzell and Peak, 1984). The economic cost of cryptic infections caused by *C. gloeosporioides* is about 25% greater than that reported for field losses (Jeger and Plumbley, 1988). Accordingly *C. gloeosporioides* has been grouped among the most important post-harvest pathogens.

In addition to its considerable detrimental economic importance, recently it has been shown that endophytic *C. gloeosporioides*, apparently nonpathogenic, is a source for production of secondary metabolites, with anticancer property (Nithya, and Muthumary, 2009). Currently, discovery and strain improvement of secondary metabolite producing fungi for industrial fermentation have gained significant interest worldwide (Zhou et al., 2010). Hence, there will be a new potential for Taxol production using improved strains of *C. gloeosporioides* in future.

Further, the *Colletotrichum* fungi are highly significant as experimental models for study of many aspects of fungal biology like development, infection process, host resistance, signal transduction, and the molecular biology of plant-pathogen interactions (The *Colletotrichum* genome database). However, very little information is

*Corresponding author E-mail:
Soltani@basu.ac.ir

available on the molecular mechanisms regulating varied pathogenicity life styles and secondary metabolite productions in these fungi and the basic tools required are only beginning to be developed by various groups.

Currently, *Agrobacterium tumefaciens*-mediated transformation (ATMT) is a powerful method for large-scale random mutagenesis, and efficiently targeted gene disruption in some fungi, based on the transfer of the T-DNA into the recipient fungal genome (Soltani et al., 2008; Soltani et al., 2009). This technique has been shown to be applicable to many filamentous fungi (Michielse et al., 2005; Soltani et al., 2008). From the first published paper on ATMT of filamentous fungi including *C. gloeosporioides* (de Groot et al., 1998), ATMT has been established as a genetic analysis tool for several other *Colletotrichum* species, i.e. *C. lagenarium* (Tsuji et al., 2003), *C. trifolii*.(Takahara et al., 2004), *C. graminicola*. (Flowers and Vaillancourt, 2005), *C. acutatum* (Talhinhas et al., 2008), *C. higginsianum* (Ushimaru et al., 2010) and *C. sansevieriae* (Nakamura et al., 2012). However, various parameters which might influence ATMT frequency of *C. gloeosporioides* have not been explored yet. A reliable insertional mutagenesis system for *C. gloeosporioides* is highly important for discovering genes involved in the pathogenesis or genes involved in the production of the anticancer compound Taxol by this species. Here, using both *hph* and *gfp*-tagged *hph* selection markers, we aimed at optimizing ATMT protocol for the efficient transformation of *C. gloeosporioides*. We further showed that this optimized ATMT resulted in producing mutants showing different phenotypic characteristics.

Materials and Methods

Fungal and bacterial strains and growth media

Colletotrichum gloeosporioides wildtype strain JSN-1389, which was isolated as a plant pathogen from Citrus species in Iran, was used as the model. Fungus strain was maintained on potato dextrose agar (PDA) medium (Merck, Darmstadt, Germany) at 28ºC. *Escherichia coli* strain XL1-blue (Stratagene) was used as a host for gene manipulations and *Agrobacterium tumefaciens* strain LBA1100 (Bundock et al., 1995) as a T-DNA donor for fungal transformation. The binary vectors pTAS10 (de Groot et al., 1998) and pBin-GFP-hph (O'Connell et al., 2004) were transferred to this strain to yield *A. tumefaciens* pSDM2312 (de Groot et al., 1998) and pBSY90 strains (this study), respectively. The *Agrobacteria* and *E.coli* strains were maintained on Luria–Bertani (LB) media (Sambrook et al., 1989) at 28ºC and 37ºC, respectively.

Fungal resistance to Hygromycin B

C. gloeosporioides JS-1389 was grown on Czapek's medium at 0, 50, 100, 150, 200, 250, 300 µg/ml hygromycin B (Sigma-Aldrich). The zone of hyphae growth of the wildtype fungus was checked daily until the colony covered the whole petri plate.

Fungal transformation

C. gloeosporioides JS-1389 was transformed using the ATMT protocol according to the method described previously (de Groot et al., 1998) as follow, with minor modifications to explore optimal conditions. Fresh *A. tumefaciens* carrying a binary vector was grown on LB medium containing 50 µg/ml kanamycin, at 28ºC overnight. The day after, it was transferred to the induction medium (IM; Bundock et al., 1995) containing 200 µM acetosyringone (AS) (Sigma–Aldrich) and grown for 6 hours. *C. gloeosporioides* JS-1389 was grown on PDA medium for 20 to 30 days to obtain a high number of conidia. 60 µl of agrobacterial suspension (OD_{620}=0.5) was mixed with 60 µl of fungal conidia (both 10^6 and 10^7 per mL). A 100 µl aliquot of the mixture was spread over Fabriano 808 or Whatman 41 (Roche Chemicals, Mannheim, Germany) filter papers on IM containing 200 µM acetosyringone. After incubation at 22ºC for 2 to 3 days, the filter papers were transferred onto PDA (for hygromycin B resistance selection) or Czapek's (for GFP-hygromycin B expression selection) selection medium containing 200 µg/ml cefotaxime (Duchefa, Netherlands) to kill the agrobacterial cells, and 100 µg/ml hygromycin B (Sigma-Aldrich) to select for fungal transformants. Stability of hygromycin resistance of transformants was tested by subculturing them five times on Czapek's media containing 100 µg/ml hygromycin B. Then, transformants were maintained on PDA. *C. gloeosporioides* JS-1389 conidial suspention, not co-cultured with *A. tumefaciens* cells but handled as described above, served as negative control. Genetic transformations of hygromycin-resistant fungal colonies were confirmed by genomic DNA analysis using PCR and fluorescence microscopy for the Gfp-tagged Hph.

Isolation of Genomic DNA

To extract DNA for Polymerase chain reaction (PCR) assays, transformants were grown on PD broth medium at room temperature for 10-15 days. A 2-5 mg mycelia of each fungal transformant was

filtered through sterile filter paper, frozen in liquid nitrogen, and grounded to a fine powder. Then DNA was extracted by the CTAB method (Zhang et al., 1996). Primers *hph*-F (5′-GCTGCGCCGATGGTTTCTACA-3′) and *hph*-R (5′-GCGCGTCTGCTGCTCCAT-3′) (Flowers,and Vaillancourt, 2005) were used to amplify a 544 bp *hph* fragment. PCR was performed with 5 µL template DNA, 1 µM each primer and Taq PCR Mix (Cinnagene) in a final volume of 25 µL. Thermocycler was programmed for one cycle of 5 min at 94 ºC, 30 cycles of 1 min at 94ºC, 1 min at 58ºC, 2 min at 72ºC, and a final cycle of 10 min at 72ºC.

Microscopy for *gfp*-tagged Hph Expression

GFP expression in the *C. gloeosporioides* transformants obtained with *A. tumefaciens* pBSY90 carrying pBin-*GFP-hph* binary vector was assessed by fluorescence microscopy. Actively growing hyphae from hygromycin resistant cultures, grown on Czapek's medium, were observed under ultraviolet light (excitation at 395–475 nm) on a Fluorescence Microscope (Bel Engineering, Italy) at 40× magnification. Wildtype isolate JS-1389 was used as the control.

Results

Hygromycin B sensitivity of *C. gloeosporioides*

In the only reported ATMT of *C. gloeosporioides*, selection of hygromycin resistant fungal transformants was performed on PDA medium as described by de Groote et al., (1998). In our experiments, addition of hygromycin B to PDA selection media resulted in variable observations. Hence, the Czapek's medium was used alternatively. The activity of hygromycin B in Czapek's medium was consistent and reliable. Consequently, inhibition of vegetation of *C. gloeosporioides* JS-1389 was assessed by growing the fungi on Czapeck's medium supplemented with hygromycin B in different concentrations, i.e. 0, 50, 100, 150, and 200 µg/ml. Growth was totally inhibited on Czapeck's medium containing 100 µg hygromycin/ml. Therefore, that concentration was considered for the selection of resistant colonies in our ATMT experiments.

Effects of experimental parameters on transformation efficiency

Transformation efficiencies were compared in experiments, in which acetosyringone (AS) was omitted from the liquid IM and the IM co-cultivation media. In agreement with most previous studies (Gouka et al., 1999; Malonek and Meinhardt 2001), inclusion of AS in the IM media was essential for the transformation of *C. graminicola*, since in the absence of AS during co-cultivation, no transformants were formed (data not shown). Co-cultivation of *C. gloeosporioides* JS-1389 conidia with *A. tumefaciens* in the presence of AS led to the formation of hygromycin-resistant fungal colonies. The transformation frequency was in the range of 70 to 120 transformants per 60 µL of 10^6 to 10^7 conidia. The average numbers of hygromycin-resistant transformants in two experiments under different conditions are shown in Table 1.

From the number of transformants produced with a given set of parameters in two experimental replications, we could conclude that some parameters had a positive effect on transformation efficiencies. A total number of 10^6 or 10^7 per mL conidia from *C. gloeosporioides* JS-1389 were co-cultivated with *A. tumefaciens* cells. As seen in Table 1, increasing the conidial concentration from 10^6 to 10^7 per mL increased ATMT in general. The previous study on ATMT of *C. gloeosporioides* has shown that 10^6 conidia per mL could result in a variable number of 50 to 130 hygromycin resistant transformants on nitrocellulose filters (de Groot *et al.*, 1998). Our data indicates that ATMT efficiency could be improved (10 to 30%) by using 10^7 conidia per mL. So, a higher number of conidia results in a higher ATMT frequency.

It is also shown that ATMT of *C. gloeosporioides* could be achieved upon 2 days of co-cultivation (de Groot et al., 1998). Here, *C. gloeosporioides* JS-1389 conidia were co-cultivated with *A. tumefaciens* cells for 2 and 3 days. As shown in Table 1, transformation efficiency was increased, 11 to 24%, after a longer (3 days) co-cultivation period. However, on the day 3, because of excessive growth of fungus and bacteria, selection of transformants was not facile.

Another experimental parameter was the choice of co-cultivation membrane. ATMT protocols usually make use of nitrocellulose filters. The only report on ATMT of *C. gloeosporioides* has introduced the efficiency of nitrocellulose filters (de Groot et al., 1998). As it is shown in Table 1, in our experiments the kind of filter paper have a relevant effect on the improvement of transformation efficiency, regardless of other parameters. Here, *C. gloeosporioides* transformants were recovered from both the Fabriano 808 and Whatman 41 membranes. Significantly, co-cultivation of Agrobacterium-*Colletotrichum* on Fabriano 808 membrane increased transformation efficiencies from 2 to 20% (Table 1).

As seen, transformation efficiencies obtained by pSDM2315 versus pBSY90 binary vector, in the same *A. tumefaciens* strain, were not significantly different. This indicates that *A. tumefaciens* LBA110 regardless of containing which plasmid , produces a similar number of transformants (Table 1). So, the binary vectors did not account for the variations we saw in transformation efficiencies.

Transformant stability

An assessment of the mitotic stability of 24 randomly selected transformants showed that they all maintained their hygromycin resistance after being sub-cultured for five generations in the presence and two generations in the absence of hygromycin on Czapeck's medium (data not shown). All 24 transformants grew when transferred onto selection media, and retained *Gfp* expression. These results demonstrated that the ATMT transformants were mitotically stable.

Confirmation of the presence of *hph* gene in genomic DNA of fungal transformants

Twenty-four transformants, which had been proved to be resistant to hygromycin B at 100 µg/ml and to retain their mitotic stability, were selected and designated in MY1 to MY24. Genomic DNA from the 24 transformants were tested for the presence of the *hph* gene by PCR using specific primers *hph*-F and *hph*-R (Fig. 1). The expected 544-bp PCR products were all detected from the 24 transformants (100%). *hph* gene product was not detected with untransformed *C. gloeosporioides* genomic DNA (Fig. 1).

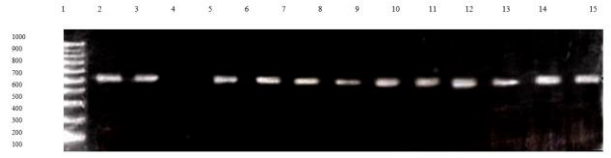

Figure 1. PCR amplification of *hph* selection marker gene (544-bp) in mitotically stable transformants (No.5-14) of *C. gloeosporioides* obtained by *A. tumefaciens* strain pSDM2315 (lanes:5-9), and by *A. tumefaciens* strain pBSY90 (lanes:10-14). Lanes 2 and 3 include positive controls (from binary vectors pTAS10, and pBin-*GFP-hph*). Lane 4 represents negative control. DNA ladder: 1000 bp ladder (Cinnagene). The observed PCR bands accord to 544 bp, as expected.

Fluorescence microscopy

To determine the stable Gfp-tagged Hph expression inside the *C. gloeosporioides* transformants, fluorescence microscopical analyses were performed on actively growing hyphae from Czapek's-hygromycin cultures. Seven out of 24 hygromycin-resistant isolates were randomely selected for fluorescence microscopy. Cells expressing a Gfp-tagged Hph protein revealed a punctuate localization pattern of this protein throughout the cell (Figure 2).

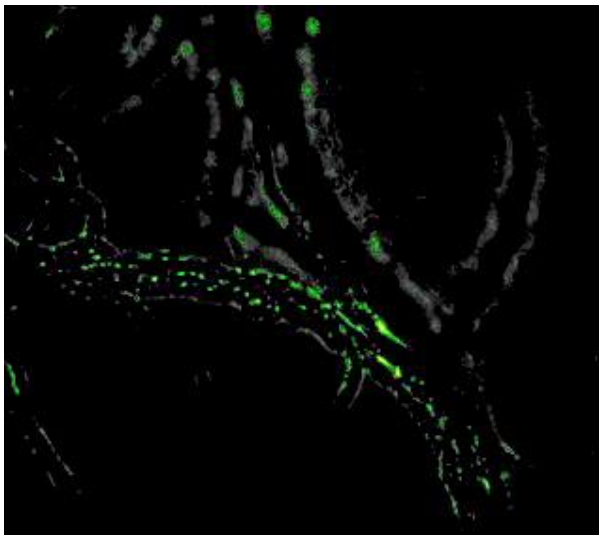

Figure 2. Gfp expression in a representative hygromycin-resistant transformant's hyphae of *C. gloeosporioides*, after ATMT with pBSY90.

Phenotypic characteristics of transformants

Seven hygromycin-resistant mutants of *C. gloeosporioides*, mycelia of which showed fluorescence illumination under microscopy experiments, were phenotypically different than their wildtype isolate *C. gloeosporioides* JSN-1389. It was observed that the rate of growth and the conidiation of transformants were increased in compared to their parental isolate (Figure. 3). Analysis of variance confirmed that vegetation of the transformants significantly differ from their parental isolate at ($P \leq 0.01$, not shown). Moreover, the color and the form of the fungal colonies on PDA plates had been changed (Figure. 3).

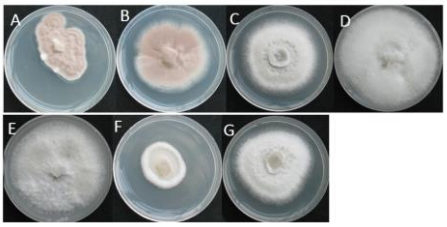

Figure 3. Different range growth and morphology/pigmentation of six *C. gloesporioides* transformants (A-F) as compared to their parental wild type (G) on PDA plates 12 days after incubation at 25ºC

Discussion

Colletotrichum gloeosporioides is of special importance in phytopathology, and more recently in pharmacology for its ability to produce anticancerous metabolites (Nithya and Muthumary, 2009). *Colletotrichum* species have haploid genomes which facilitates molecular genetic approaches, such as gene targeting and insertional mutagenesis. *C. gloeosporioides* genome is not sequenced yet. For functional genetics of this fungus in order to discover the genes involved in the pathogenesis, or the genes involved in the production of the anticancer compound, Taxol, by this species, a reliable insertional mutagenesis system is highly important. Restriction Enzyme-Mediated DNA Integration (REMI) and Polyethylene Glycol (PEG) genetic transformation protocols have several drawbacks for fungal transformation, but *A. tumefaciens*-mediated transformation has several advantages over these methods (Michielse et al., 2005; Soltani et al., 2008) such as stable transformants with a single-copy integrated DNA.

Agrobacterium tumefaciens-mediated transformation of several *Colletotrichum* species has been reported before (de Groot et al., 1998; Tsuji et al., 2003; Takahara et al., 2004; Flowers and Vaillancourt, 2005; Talhinhas et al., 2008; Ushimaru et al., 2010; Nakamura et al., 2012). Here, we aimed at exploring the optimal conditions for *A. tumefaciens*-mediated transformation of *C. gloeosporioides* using *hph* and *gfp* genes as selection markers, as well as initial assessment of possibility of ATMT for insertional mutagenesis of this fungus. Results showed that for ATMT falcate spores can be used instead of protoplasts. Several experimental parameters were shown to affect transformation efficiencies, i.e. the length of co-cultivation, the ratio of fungal conidia to bacterium during co-cultivation, the kind of membrane during co-cultivation and the kind of fungal growth medium during transformant selection showed the highest influences on ATMT frequencies. Our results indicate that the optimal ATMT of *C. gloeosporioides* is achieved after 3 days of co-cultivation, at 10^7 per mL fungal conidia, via the use of Fabriano 808 filter paper and Czapek's culture medium. It was already shown that after 2 days of co-cultivation of *A. tumefaciens* with 10^6 per mL *C. gloeosporioides* conidia could result in a variable number of 50 to 130 hygromycin resistant transformants on nitrocellulose filters (de Groot et al., 1998). Here, it is shown that fabriano filters, and Czapek;s medium have improved the reliability of the protocol. Moreover, successive subculturing of transformants on selective and non-selective media demonstrated the stable expression of transgens as already seen for ATMT (Soltani et al., 2008). PCR analysis revealed the presence of transferred genes, and flourescence microscopy showed the expression of Gpf-tagged Hph protein inside the fungal hyphae. This finding suggests a possibility for subcellular localization of fungal Gfp-tagged proteins. The obtained insertional mutants varied in their growth rate, conidiation, color and shape, as compared with their parental wildtype isolate. This suggests the applicability of this technique for functional genetic analysis of *C. gloeosporioides* through insertional mutagenesis. Further research on the molecular mechanisms regulating varied pathogenicity life styles and secondary metabolite productions in *C.*

Table.1. Effect of different parameters (time, paper, number of conidia) during co-cultivation at 22ºC, as well as the *A.tumefacience* strains used for ATMT on *Colletotrichum gloeosporioides* JS-1389 on the number of hygromycin-resistant transformants.

Co-cultivation parameters			*A.tumefaciens* strain	
Conidia cell/mL	membrane	Days	pSDM2315	pBSY90
			number of hygromycin-resistant transformants per 60 µL conidia	
1×10^6	F	2	80	77
1×10^7	F	2	96	89
1×10^6	w	2	71	70
1×10^7	w	2	88	79
1×10^6	f	3	98	85
1×10^7	f	3	119	111
1×10^6	w	3	83	83
1×10^7	w	3	99	92

f) Fabriano 808, w) Watman 41
Data are averages of 2 independent experiments.

gloeosporioides will shed light on the hidden secrets of this fungus.

Acknowledgments

We wish to thank Prof. Dr. P. J. J. Hooykaas, (Institute of Biology, Leiden University, The Netherlands) for kindly providing *Agrobacterium* strain and the pTAS10 binary vector. We are also grateful to Prof. Dr. R.J. O'Connell (Max-Planck-Institute for Plant Breeding Research, Cologne, Germany) for his generous providing pBin-*GFP-hph* binary vector. Fluorescence microscopy unit of Shiraz Medical University, Iran, is appreciated for their microscopy service. We thank also Maghsoud Seifi for his technical assistance. This work was financed by the Ministry of Science, Research, and Technology of Iran.

References

1. Bundock P., Dulk-Ras A., Beijersbergen A. and Hooykaas P. J. (1995) Trans-kingdom T-DNA transfer from *Agrobacterium tumefaciens* to *Saccharomyces cerevisiae.* EMBO Journal, 14: 3206–3214.
2. Damm, U., Barroncelli, R., Cai, L., Kubo, Y., O'Connell, R., Weir, B., Yoshino, K., and Cannon, P. F. (2010) *Colletotrichum*: species, ecology and interactions. IMA Fungus, 1: 161–165.
3. de Groot, M.J., Bundock, P., Hooykaas, P.J.J, and Beijersbergen, A.G. (1998) *Agrobacterium tumefaciens*-mediated transformation of filamentous fungi. Nat Biotechnol, 16: 839-842.
4. Freeman, S., and Shabi, E. (1996) Cross-infection of subtropical and temperate fruits by Colletrotrichum species from various hosts. Physiol Mol Plant Pathol, 49: 395–404.
5. Fitzell, R. D., and Peak, C. M. (1984) The epidemiology of anthracnose disease of mango: inoculum sources, spore production and dispersal. Ann Appl Biol, 104: 53–59.
6. Flowers, J. L., Vaillancourt, L.J. (2005) Parameters affecting the efficiency of *Agrobacterium tumefaciens*-mediated transformation of *Colletotrichum graminicola*. Curr Genet, 48: 380-388.
7. Gouka, R., Gerk C., Hooykaas, P. J. J., Bundock, P., Musters, W., Verrips, C., and de Groot, M. (1999). Transformation of *Aspergillus awamori* by *Agrobacterium tumefaciens*-mediated homologous recombination. Nat Biotechnol 17: 598–601.
8. Jeger, M.J. and Plumbley, R.A. (1988) Post-harvest losses caused by anthracnose (Colletotrichum gloeosporioides) of tropical fruits and vegetables. Biodeterioration 7: 642–646.
9. Malonek, S., and Meinhardt, F. (2001) *Agrobacterium tumefaciens*-mediated genetic transformation of the phytopathogenic ascomycete *Calonectria morganii*. Curr Genet 40: 152–155.
10. Michielse, C. B., Hooykaas, P. J. J., Hondel, C. A. M. J. J. van den, and Ram, A. F. J. (2005) Agrobacterium-mediated transformation as a tool for functional genomics in fungi. Curr Genet, 48: 1-17.
11. Iwai H. (2012) *Agrobacterium tumefaciens*-mediated transformation for investigating pathogenicity genes of the phytopathogenic fungus *Colletotrichum sansevieriae*. Curr Microbiol, 65: 176-182.
12. Nithya, K., and Muthumary, J. (2009). Growth studies of *Colletotrichum gloeosporioides* (Penz.) Sacc. - a taxol producing endophytic fungus from *Plumeria acutifolia*. Ind J Sci Technol, 6 :14-19.
13. O'Connell, R., Herbert, C., Sreenivasaprasad, S., Khatib. M., Esquerre-Taguye, M. T., and Damus, B. (2004) A novel Arabidopsis-*Colletotrichum pathosystem* for the molecular dissection of plant-fungal interactions. Mol Plant-Microbe Interact, 17: 272-282.
14. Sambrook, J., Fritsch E., F., and Maniatis, T. (1989) Molecular Cloning: A Laboratory Manual. Cold Spring Harbor Laboratory Press; Plainview, NY.
15. Soltani, J., van Heusden, G.P.H., and Hooykaas, P.J.J. (2009) Deletion of host histone acetyltransferases and deacetylases strongly affects Agrobacterium-mediated transformation of *Saccharomyces cerevisiae*. FEMS Microbiol Lett, 298: 228-233.
16. Soltani, J., van Heusden, G.P.H. and Hooykaas, P.J.J. (2008) Agrobacterium-mediated transformation of non-plant organisms. In Agrobacterium: from biology to biotechnology. pp 649-675. Edited by Tzfira, T. and Citovsky, V. Springer press. New York, USA.
17. Takahara, H., Tsuji, G., Kubo, Y., Yamamoto, M., Toyoda, K., Inagaki, Y., Ichinose, Y. and Shiraishi, T. (2004) *Agrobacterium tumefaciens*-mediated transformation as a tool for random mutagenesis of *Colletotrichum trifolii*. J Gen Plant Pathol, 70: 93–96.
18. Talhinhas, P., Muthumeenakshi, S., Neves-Martins, J., Oliveira, H., and Sreenivasaprasad, S. (2008). Agrobacterium-mediated transformation and insertional mutagenesis in *Colletotrichum acutatum* for investigating varied pathogenicity lifestyles. Mol Biotechnol, 39: 57–67.
19. Tsuji, G., Fujii, S., Fujihara, N., Hirose, C., Tsuge, S., Shiraishi, T., and Kubo, Y. (2003) *Agrobacterium tumefaciens*-mediated transformation

for random insertional mutagenesis in *Colletotrichum lagenarium*. J Gen Plant Pathol, 69: 230-239.

20. Ushimaru, T., Terada, H., Tsuboi, K., Kogou, Y., Sakaguchi, A., Tsuji, G., and Kubo, Y. (2010). Development of an efficient gene targeting system for *Colletotrichum higginsianum* using a non-homologousend-joining mutant and *Agrobacterium tumefaciens*-mediated gene transfer. Mol Genet Genomics, 284: 357–371

21. Waller, J. M. (1992). *Colletotrichum* disease of perennial and other cashcrops, in *Colletrotrichum*, biology, pathology and control, ed by Bailey J.A. and Jeger M.J., CAB International, Wallingford, UK,pp 167–185.

22. Zhang, D., Yang, Y., Castlebury, L. A., and Cerniglia, C. E. (1996) A method for the large scale isolation of high transformation efficiency fungal genomic DNA. FEMS Microbiol Lett, 145: 261–265.

23. Zhou, X., Zhu, H., Liu,L., Lin, J., Tang,K. (2010). Recent advances and future prospects of taxol-producing endophytic fungi. Appl Microbiol Biotechnol, 86: 1707–1717.

The *in vitro* effects of $CoCl_2$ as ethylene synthesis inhibitor on PI based protein pattern of potato plant (*Solanum tuberosum* L.)

Marzieh Taghizadeh and Ali Akbar Ehsanpour*

Department of Biology, Faculty of Science, University of Isfahan, Isfahan, Iran

Received 10 August 2013 Accepted 14 September 2013

Abstract

The effect of $CoCl_2$ as an ethylene synthesis inhibitor on changes of protein pattern was investigated in potato (*Solanum tuberosum L.*) plants cultivar White Desiree. In vitro grown plants were subjected to MS medium containing 0, 5, 10, 15, 20, 30, 40 and 60 mg/l $CoCl_2$ for 4 weeks. Different concentrations of $CoCl_2$ showed significant effect on the total soluble proteins. Among different concentrations of $CoCl_2$, using 20 mg/l $CoCl_2$ was the best concentration to inhibit ethylene formation and induce potato plant growth. Application of $CoCl_2$ in the culture medium changed the total protein as well as SDS-PAGE and Iso-electric Point Electrophoresis (PI) patterns. Protein pattern in potato tuber did not show any detectable changes.

***Keywords*:** potato, $CoCl_2$, ethylene, protein pattern

Introduction

The potato (*Solanum tuberosum L.*) is one of the most valuable crop species belonging to the Solanaceae family (Orczyk et al., 2003). The growth and development of potato is sensitive to accumulation of ethylene under *in vitro* culture condition. Ethylene (C_2H_4) is a simple Plant growth regulator which is involved in the regulation of many aspects of plant growth and development and plays a major role in the ripening of climacteric fruits, plant defense, abscission (Dupille et al., 1993). Accumulation of ethylene in in vitro culture induces growth abnormalities such as production and development of stoloniferous shoots, small leaves and root generation from stem during short and long-term period tissue culture of potato explants (Sarkar et al., 2002; Sarkar et al., 1999). The negative effects of ethylene on plants under *in vitro* culture can be controlled using cobalt chloride ($CoCl_2$) as an ethylene inhibitor biosynthesis. The ethylene biosynthesis pathway is often started from methionine (Met) and then produces S-adenosylmethionine (SAM), 1-aminocyclopropane-1-carboxylic acid (ACC) and finally ethylene (Adams and Yang, 1979). The final step in the biosynthesis of ethylene is catalyzed by an ethylene-forming enzyme or ACC oxidase, which is responsible for the conversion of ACC to ethylene (Yang and Hoffman, 1984). ACC oxidase is a member of the ferrous ion-dependent family of non-haeme oxygenizes (Barlow et al., 1997). Ethylene inhibitors can be divided into two categories. The first one refer to those acting on the ethylene receptors, such as $AgNO_3$ and the second one refers to ethylene biosynthesis, such as $CoCl_2$. Cobalt is an essential element for humans and animals. In plants, it is not essential but beneficial for their growth. Excess CO is also toxic to plants (Nagpal, 2004).

Proteins are compounds of fundamental importance for all functions in the cell (Dose, 1980). It is well known that alteration of gene expression is always involved in plants under specific culture condition. Protein variation is an essential part of plant response to stress as well as for adaptation to environmental conditions (Hieng et al., 2004). Proteins are final products of informational pathways in cells that produce in response to cellular needs and transfer to proper locations in cells. Previous studies demonstrated that application of STS and Nano silver (Rostami and Ehsanpour, 2009) on potato (*Solanum tuberosum L.*) prevented the ethylene accumulation, and changed the protein pattern were detected by SDS-PAGE. However, so far information about changes in protein pattern of potato plants using SDS-PAGE and PI is not available. The present study was carried out to understand how potato plant cell dose react to inhibition of ethylene biosynthesis and presence of cobalt in the plant.

*Corresponding author E-mail: ehsanpou@sci.ui.ac.ir

Materials and Methods

Plant material and culture conditions

Potato explants (*Solanum tuberosum L.*) cultivar White Desiree was propagated on MS medium (Murashig and Skoog, 1962) supplemented with silver thiosulfate (STS, 50 µM), agar (1% w/v), sucrose (3% w/v) and pH 5.8. Auxiliary buds from in vitro propagated plants were transferred to the above mentioned medium containing 0 (control), 5, 10, 15,20,30,40 and 60 mg/L $CoCl_2$ without STS. All cultures then were kept in the culture room with a 16/8 hour (light/dark) photoperiod at 25±2ºC for 4 weeks.

Leaf protein extraction

Approximately 0.2 gram of fresh stem-leaf from 4-week-old plants and potato tuber were homogenized in liquid nitrogen, then protein was extracted using extraction buffer (50mM Tris- HCl, 1mM DTT, 2mM EDTA, 2mM 2-Mercaptoethanol, pH 7.5. For extraction of proteinsm buffer was modified as 1mM PMSF at pH 7.2 according to the method described by Amini et al., (2007). For separation of proteins based on their PI, total extracted proteins then were precipitated and purified in a buffer with single pH ranging from 2 to 10, based on Patent No. 89/4217, Tehran, Iran.

The concentration of total soluble proteins from leaf samples were determined according to modified Bradford (1976) method, using bovin serum albumin (BSA) as standard. SDS-PAGE and PI were performed using 12% separating and 5% stacking gels. After electrophoresis at 100V, protein bands were stained using Coomassie brilliant blue and silver nitrate and finally relative density of protein bands with remarkable changes was analyzed.

All experiments were carried out in three replications. Data were subjected to ANOVA and the mean differences were compared by Dunkan test at $P<0.05$.

Results

The effect of $CoCl_2$ on total protein level

Increase at protein level of leaf-stem at concentrations of 20, 30, 40 and 60 mg/L $CoCl_2$, compared to the control samples, was observed (Fig 1). It was shown that concentration of 20 mg/L $CoCl_2$ increased protein content compared to the other treatments.

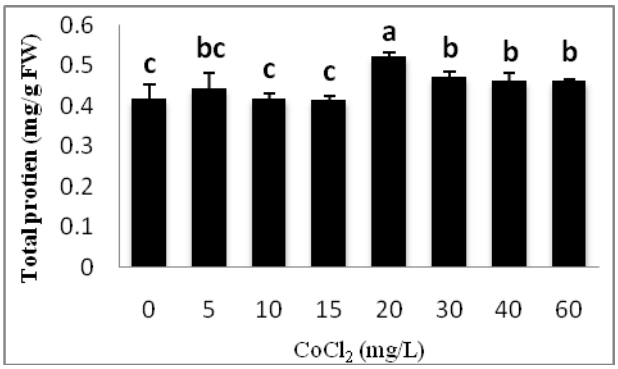

Fig. 1. The effect of $CoCl_2$ on the total protein level of leaf-stem of potato plants. Uncommon letters indicate the significant differences ($P<0.05$).

The effect of $CoCl_2$ on protein patterns production in leaf-stem of potato by PI and SDS-PAGE:

The total protein of explants in leaf-stem parts and potato plants in concentrations of 0 and 20 mg/L $CoCl_2$ were extracted and used for electrophoresis by SDS-PAGE and PI.

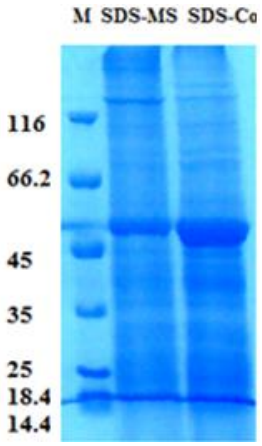

Figure 2. The SDS-PAGE (pH 7) protein pattern extracted from stem-leaf treated with $CoCl_2$ (+Co) and untreated (-Co), M: Marker

Proteins pattern from stem-leaf using SDS-PAGE revealed no difference between treated and untreated plants. However, there were obvious differences in either severity of some protein expressions (both increase and decrease) or expression of some proteins under experimental conditions. In electrophoresis by PI method, the protein solutions resulted from two optimized concentration of 0 and 20 mg $CoCl_2$ (data not shown) at pH ranging from 2 to 12, were separated and protein precipitated at a specific pH was loaded

on the SDS-PAGE gel. The intensity of protein bands in acidic and some neutral pH were more than that of protein bands in alkaline pH. As shown in figure 2, the intensity of protein bands in pH 2 was lower compared to the other pH. There was no counterparts for band 1 (Approx.116 KD), band 2 (Approx. 70KD) and bond 3 (Approx. 65KD) in pH 2 in the control as well as 20 mg/L $CoCl_2$. However, the expression intensity of band 4 (Approx. 50KD) at 20 mg/L $CoCl_2$ was increased compared to the untreated plants as shown in Figure 2. When proteins were separated using PI, at pH 3, the intensity of protein bands compared to pH 2 was increased. Moreover, band 2 and band 3 were observed in cobalt treated plants compared to the control plants (Figure 3 and 4).

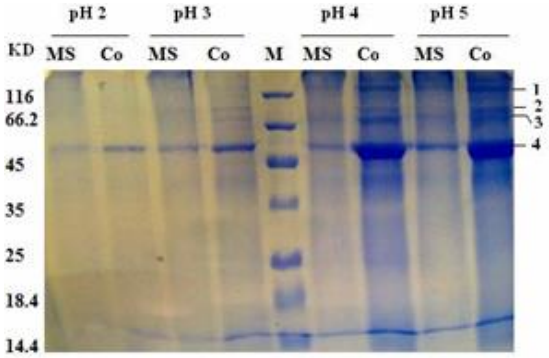

Fig. 3. The effect of CoCl2 on protein pattern at pH 2, 3, 4, and 5 (MS: control, Co: 20 mg/l CoCl2)

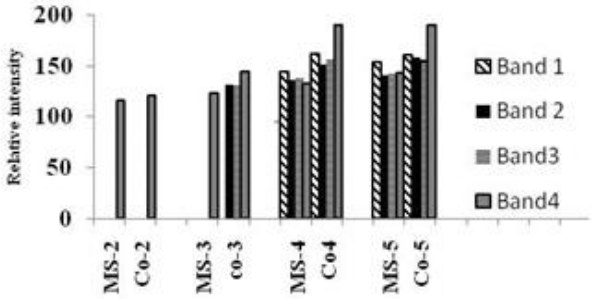

Fig. 4. The effect of CoCl2 on relative intensity of protein bands at pH: 2, 3, 4 and 5

There was an increase in intensity of protein bands at pH 4 and in particular pH 5 compared to the other pH. Band 1, band 2, band 3, and band 4, had more intensity in treated plants with cobalt. In this pH, also, more bands were observed compared to the control and other pH. At pH 6 and pH 7 (Figure 5 and 6), band 1 and band 4 in cobalt treated plants had higher expression levels and bands 2 and 3 were absent (Fig. 4 and 5). At pH 10-12 (Figure 7), there was a considerable decrease in protein bands. At higher alkaline pH, the intensity of protein bands decreased more. Bands 2 and 3 were absent and the intensity of band 1 did not change significantly

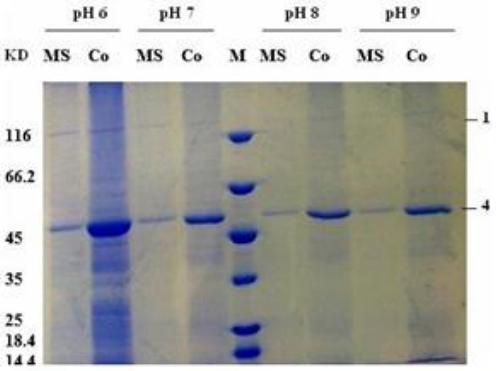

Fig. 5: The effect of CoCl2 on protein patterns pH: 6, 7, 8 and 9 (MS: control, Co: 20 mg/l CoCl2).

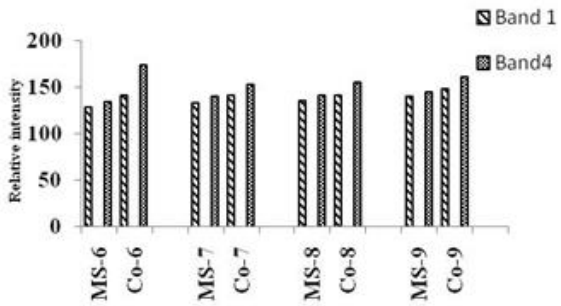

Fig.6. The effect of CoCl2 on relative intensity of protein bands at pH 6, 7, 8 and 9.

compared to the controls (Figure 8). However, the intensity of band 2 at 20 mg/l $CoCl_2$ increased much higher compared to the controls. As figure 9 shows when protein pattern of the tuber were analyzed by SDS PAGE, no obvious changes were observed either in treated or untreated plants with cobalt.

Discussion

Treatment of potato plants with cobalt induced some changes in total soluble proteins of stem-leaf explants of potato cultivar White Desiree. In our experiments 20, 30, 40, 60 mg/L $CoCl_2$ increased protein content of the potato leaf and stem. The protein content changes might be due to the ethylene biosynthesis inhibition or as a result of changes in physiology and metabolism of potato plant cells responded to cobalt as a heavy metal (Clemens, 2006). We need to confirm the possible cobalt function in details in the future.

If looking at the cobalt as a heavy metal, cobalt can change the total protein by altering the expression level of some proteins to protect plant

cells against toxicity effects. Normally, organisms apply several ways to detoxify heavy metals. One of the more general ways is to synthesize cyctein-rich proteins and peptides known as phytoklatines (Clemens, 2006). Whether the increased proteins in the present study include phytoklatines is increased needs to be studied in the future. Furthermore, the production of reactive oxygen species (ROS) is one the biochemical changes due to the heavy metals (e.g. cobalt) responses to plant (Cho and Park, 2000). Antioxidant enzymes such as superoxide dismutase (SOD), peroxidase and catalase (CAT) play an important role in defending these toxic compounds (Gupta et al., 2002).

When proteins are separated on the basis of molecular weight using SDS PAGE, distinctive protein bands were revealed on the gel. It has been reported that, heavy metals including (cobalt) are able to change the plant protein production patterns (Ewais, 1997). The bands obtained by this way may be representative of a series of proteins with more or less similar molecular weight only. In other words, SDS PAGE does not show any other information from the separated proteins on the gel. In contrast, two dimensional electrophoresis (2DE) method illustrates more details of the proteins. In fact by using 2DE it is possible to identify a single protein spot and discuss the actual changes of protein expression in details in the plant cells exposed to heavy metals. In the present study for the first time we are presenting some data in which proteins first separated based on the specific PI and the isolated proteins were loaded on the SDS-PAGE gel. In fact this method of isolation is simple 2DE with some differences with the actual 2DE, protein bands in this way show 2 characters including molecular weight as well as PI. In the present study protein bands were separated within ranges of pH from 2 to 10. In this study a few protein bands in particular those with approximately 55 kD, were low in acidic PI while much higher in basic PI. Also the molecular weight of particular this protein almost was constant in the pH 2-10 but whether this is a single protein, separated in different ranges of pH or different proteins with similar molecular weight is unknown. Since, large subunit of RuBisCo enzyme is about 55 KD (Dhingra et al., 2004), it can be suggested that protein band with 55 KD might be RuBisCo enzyme.

The protein pattern of the potato tuber on SDS-PAGE did not reveal any change, suggesting no effect or very low effect of cobalt on tubers. In our previous data, we found that no cobalt was detectable in potato tuber tissue (data not shown). Consequently, it is acceptable to assume that cobalt has no effect on protein changes in the tuber.

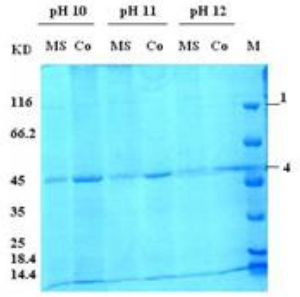

Fig.7. The effect of CoCl2 on protein patterns at pH 10, 11 and 12 (MS: control, Co: 20 mg/l CoCl2).

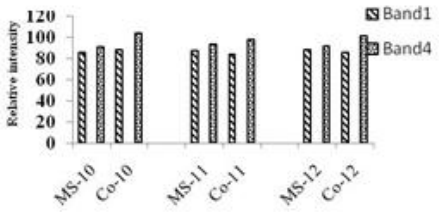

Fig. 8. The effect of CoCl2 on relative intensity of protein bands at pH 10, 11 and 12.

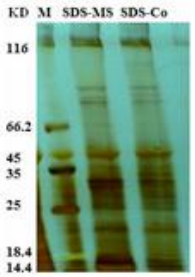

Fig. 9. The effect of CoCl2 on potato tuber protein pattern using SDS-PAGE. (MS: control, Co: 20 mg/l CoCl2).

Acknowledgment

The authors gratefully acknowledge the University of Isfahan for their support.

References

1-Adams D. O. and Yang S. F. (1979) Ethylene biosynthesis – identification of 1-aminocyclopropane-1-carboxylic acid as an intermediate in the conversion of methionine to ethylene. Proceedings of the National Academy of Sciences 76: 170-174.

2- Amini F., Ehsanpour A. A., Hoang Q. T. and Shin J. Sh. (2007) Protein pattern changes in tomato under *in vitro* salt stress. *Russian Journal*

of Plant Physiology 54: 464-471.
3- Barlow J. N., Zhang Z., John P., Baldwin J. and Schofield C. J. (1997) Inactivation of 1-aminocyclopropane-1-carboxylic acid involves oxidative modifications. Biochemistry 36: 3563–3569.
4- Bradford M. (1976) A rapid and sensitive method for the quantitation of microgram quantities of protein utilizing the principle of protein-dye binding. Anal of Biochemistry 72: 248-254.
5- Brooks S. C., Herman J. S., Hornberger G. M. and Mills A. L. (1998) Biodegradation of cobalt–citrate complexes: Implications for cobalt mobility in groundwater. Journal of contaminant hydrology 32: 99-115.
6- Cho U. H. and Park J. O. (2000) Mercury-induced oxidative stress in tomato seedlings. Plant Science 156: 1-9.
7- Clemens S. (2006) Evolution and function of phytochelatin synthases. Journal of plant physiology 163: 319-332.
8- Dhingra A., Portis A. R, Daniell H. (2004). Enhanced translation of a chloroplast-expressed RbcS gene restores small subunit levels and photosynthesis in nuclear RbcS antisense plants. *Proc. Natl. Acad. Sci. U.S.A.* **101** (16): 6315–20.
8- Dose K. (1980) Biochemie. Springer Berlin, Heidelberg, New York.
9- Dupille E., Rombaldi C., Lelievre J. M., Cleyet-Marel, J. C., Pech J. C. and Latche A. (1993) Purification, properties and partial amino-acid sequence of 1-aminocyclopropane-1-carboxylic acid oxidase from apple fruits. Planta 190: 65–70.
10- Ewais E. (1997) Effects of cadmium, nickel and lead on growth, chlorophyll content and proteins of weeds. Biologia Plantarum 39: 403-410.
11- Gupta M., Cuypers A., Vangronsveld J. and Clijsters H. (2002) Copper affects the enzymes of the ascorbate-glutathione cycle and its related metabolites in the roots of *Phaseolus vulgaris*. Physiologia Plantarum 106: 262-267.
12- Hieng B., Ugrinovich K., Sustar-Vozlich J. and Kidric M. (2004) Different classes of proteases are involved in the response to drought of *Phaseolus vulgaris* cultivars differing in sensitivity. Journal of Plant Physiology 161**:** 519-530.
13- Murashige T. and Skoog F. (1962) A revised medium for rapid growth and bioassays with tobacco tissue cultures. *Physiologia Plantarum* 15**:** 473-497.
14- Orczyk W., Przetakiewicz J. and Nadolska-Orczyk A. (2003) Somatic hybrids of *Solanum tuberosum*–application to genetics and breeding. Plant Cell, Tissue and Organ Culture 74: 1-13.
15- Reeves R. D., Baker A. J. M., Borhid A. and Berazain R. (1999) Nickle hyperaccumulation in the serpentine flora of Cuba. Annals of Botany 83.29-38.
16- Rostami F. and Ehsanpour A. (2009) Application of Silver Thiosulphate (STS) on silver Accumulation and protein pattern of potato under *in vitro* culture. Malaysia Application of Biology 38: 49-54.
17- Sarkar D., Kaushik S. and Naik P. (1999) Minimal growth conservation of potato microplants: silver thiosulfate reduces ethylene-induced growth abnormalities during prolonged storage *in vitro*. Plant Cell Reports 18: 89-93.
18- Sarkar D., Sud K. C., Chakrabarti S. K. and Naik P. S. (2002) Growing of potato microplants in the presence of algainare- silver thiosulphate capsules reduces rthylene- induced culture abnormalities during minimal growth conservation in vitro. Plant Cell, Tissue and Organ Culture 68: 79-89.
19- Yang S. F. and Hoffman N. E. (1984) Ethylene biosynthesis and its regulation in higher plants, Annu. Rev. Plant Physiol 135: 155–189.

Scientific Reviewers

MANUSCRIPT PREPARATION

Manuscripts should be prepared in accordance with the uniform requirements for Manuscript's Submission to **"Journal of Cell and Molecular Research".**

Language: Papers should be in English (either British or American spelling). The past tense should be used throughout the results description, and the present tense in referring to previously established and generally accepted results. Authors who are unsure of correct English usage should have their manuscript checked by somebody who is proficient in the language; manuscripts that are deficient in this respect may be returned to the author for revision before scientific review.

Typing: Manuscripts must be typewritten in a font size of at least 12 points, double-spaced (including References, Tables and Figure legends) with wide margins (2.5 cm from all sides) on one side of the paper. The beginning of each new paragraph must be clearly indicated by indentation. All pages should be numbered consecutively at the bottom starting with the title page.

Length: The length of research articles should be restricted to ten printed pages. Short communication should not exceed five pages of manuscript, including references, figures and tables. Letters should be 400-500 words having 7-10 references, one figure or table if necessary. Commentaries and news should also be 800-1000 words having 7-10 references and one figure or table if necessary.

Types of Manuscript: JCMR is accepting original research paper, short communication reports, invited reviews, letters to editor, biographies of scientific reviewers, commentaries and news.

GENERAL ARRANGEMENT OF PAPERS

Title: In the first page, papers should be headed by a concise and informative title. The title should be followed by the authors' full first names, middle initials and last names and by names and addresses of laboratories where the work was carried out. Identify the affiliations of all authors and their institutions, departments or organization by use of Arabic numbers (1, 2, 3, etc.).

Footnotes: The name and full postal address, telephone, fax and E-mail number of corresponding author should be provided in a footnote.

Abbreviations: The Journal publishes a standard abbreviation list at the front of every issue. These standard abbreviations do not need to be spelled out within paper. However, non-standard and undefined abbreviations used five or more times should be listed in the footnote. Abbreviations should be defined where first mentioned in the text. Do not use abbreviations in the title or in the Abstract. However, they can be used in Figures and Tables with explanation in the Figure legend or in a footnote to the Table.

Abstract: In second page, abstract should follow the title (no authors' name) in structured format of not more than 250 words and must be able to stand independently and should state the Background, Methods, Results and Conclusion. Write the abstract in third person. References should not be cited and abbreviations should be avoided.

Keywords: A list of three to five keywords for indexing should be included at bottom of the abstract. Introduction should contain a description of the problem under investigation and a brief survey of the existing literature on the subject.

Materials and Methods: Sufficient details must be provided to allow the work to be repeated. Correct chemical names should be given and strains of organisms should be specified. Suppliers of materials need only be mentioned if this may affect the results. Use System International (SI) units and symbols.

Results: This section should describe concisely the rationale of the investigation and its outcomes. Data should not be repeated in both a Table and a Figure. Tables and Figures should be selected to illustrate specific points. Do not tabulate or illustrate points that can be adequately and concisely described in the text.

Discussion: This should not simply recapitulate the Results. It should relate results to previous work and interpret them. Combined Results and Discussion sections are encouraged when appropriate.

Acknowledgments: This optional part should include a statement thanking those who assisted substantially with work relevant to the study. Grant support should be included in this section.

References: References should be numbered and written in alphabetical order. Only published, "in press" papers, and books may be cited in the reference list (see the examples below). References to work "in press" must be accompanied by a copy of acceptance letter from the journal. References should not be given to personal communications, unpublished data, manuscripts in preparation, letters, company publications, patents pending, and URLs for websites. Abstracts of papers presented at meetings are not permissible. These references should appear as parenthetical expressions in the text, e.g. (unpublished data). Few example of referencing patterns are given as follows:

Bongso A., Lee E. H. and Brenner S. (2005) Stem cells from bench to bed side. World Scientific Publishing Co. Singapore, 38-55 pp.

Haddad F., Gholami V. and Pirayesh Shirazi Nejad M. (2009) Ozone inhalation can induce chromosomal abnormalities in bone marrow cells of Wistar rats. Ferdowsi University International Journal of Biological Sciences 1: 41-46.

Note: All the references should be in EndNote format (JCMR EndNote Style is available on JCMR's web site)

Tables and Figures: Tables and Figures should be numbered (1, 2, 3, etc.) as they appear in the text. Figures should preferably be the size intended for publication. Tables and Figures should be carefully marked. Legends should be typed single-spaced separately from the figures. Photographs must be originals of high quality. Photocopies are not acceptable. Those wishing to submit color photographs should contact the Editor regarding charges.

Page charges: There is no page charge for publication in the Journal of Cell and Molecular Research.

Table of Contents

Journal of Cell and Molecular Research

Volume 5, Number 1, Summer 2013